NORSAR Scientific Report No. 2-2010

Semiannual Technical Summary

1 January - 30 June 2010

Frode Ringdal (ed.)

Kjeller, August 2010

REPORT DOCUMENTATION PAGE

Form Approved
OMB No. 0704-0188

1. REPORT DATE *(DD-MM-YYYY)*	2. REPORT TYPE	3. DATES COVERED *(From - To)*
15-08-2010	Semiannual Technical Summary	1 January - 30 June 2010

4. TITLE AND SUBTITLE
Semiannual Technical Summary, 1 January - 30 June 2010

5a. CONTRACT NUMBER
FA2521-06-C-8003

5b. GRANT NUMBER

5c. PROGRAM ELEMENT NUMBER
NDC Support / R&D

6. AUTHOR(S)
Frode Ringdal (Ed.)

5d. PROJECT NUMBER
T/6110

5e. TASK NUMBER
SOW Task 4.2 & 4.3

5f. WORK UNIT NUMBER
CDRL sequence nos. A001-A004

7. PERFORMING ORGANIZATION NAME(S) AND ADDRESS(ES)
Stiftelsen NORSAR
Post Box 53
NO-2027 Kjeller
Norway

8. PERFORMING ORGANIZATION REPORT NUMBER
Scientific Report No. 2-2010

9. SPONSORING/MONITORING AGENCY NAME(S) AND ADDRESS(ES)
AFTAC/TTS, 1030 South Highway A1A MS 1000, Patrick AFB, FL 32925-3002

Army Space and Missile Defense Command , 1515 Wilson Blvd., Suite 720
Arlington, VA 22209

10. SPONSOR/MONITOR'S ACRONYM(S)
AFTAC/TTS & USASMDC

11. SPONSOR/MONITOR'S REPORT NUMBER(S)

12. DISTRIBUTION/AVAILABILITY STATEMENT
Approved for public release; distribution unlimited

13. SUPPLEMENTARY NOTES

14. ABSTRACT

This report describes activities carried out at NORSAR under Contract No. FA2521-06-C-8003 (T/6110) for the period 1 January - 30 June 2010. In addition, it provides summary information on operation and maintenance (O&M) activities at the Norwegian National Data Center (NDC) during the same period. The O&M activities, including operation of transmission links within Norway and to Vienna, Austria, are being funded jointly by the CTBTO/PTS and the Norwegian Government, with the understanding that the funding of O&M activities for primary stations in the International Monitoring System (IMS) will gradually be transferred to the CTBTO/PTS. The O&M statistics presented in this report are included for the purpose of completeness, and in order to maintain consistency with earlier reporting practice. Some of the research activities described in this report are funded by the United States (cont.)

15. SUBJECT TERMS
NORSAR, Norwegian Seismic Array

16. SECURITY CLASSIFICATION OF:			17. LIMITATION OF ABSTRACT	18. NUMBER OF PAGES	19a. NAME OF RESPONSIBLE PERSON
a. REPORT	b. ABSTRACT	c. THIS PAGE			Mr. Kyle S. Roberts, AFTAC/TTX
U	U	U	SAR	77	19b. TELEPHONE NUMBER *(Include area code)* (321) 494-9471

Reset

Standard Form 298 (Rev. 8/98)
Prescribed by ANSI Std. Z39.18

Abstract (cont.)

Government, and the United States also covers the cost of transmission of selected data from the Norwegian NDC to the United States NDC.

The seismic arrays operated by NOR-NDC comprise the Norwegian Seismic Array (NOA), the Arctic Regional Seismic Array (ARCES) and the Spitsbergen Regional Array (SPITS). This report presents statistics for these three arrays as well as for additional seismic stations which through cooperative agreements with institutions in the host countries provide continuous data to NOR-NDC. These additional stations include the Finnish Regional Seismic Array (FINES) and the Hagfors array in Sweden (HFS).

The NOA Detection Processing system has been operated throughout the period with an uptime of 100%. A total of 2,087 seismic events have been reported in the NOA monthly seismic bulletin during the reporting period. On-line detection processing and data recording at the NDC of data from ARCES, FINES, SPITS and HFS data have been conducted throughout the period. Processing statistics for the arrays for the reporting period are given.

A summary of the activities at the NOR-NDC and relating to field installations during the reporting period is provided in Section 4. Norway is now contributing primary station data from two seismic arrays: NOA (PS27) and ARCES (PS28), one auxiliary seismic array SPITS (AS72), and one auxiliary three-component station JMIC (AS73). These data are being provided to the IDC via the global communications infrastructure (GCI). Continuous data from the three arrays are in addition being transmitted to the US NDC. The performance of the data transmission to the US NDC has been satisfactory during the reporting period.

So far among the Norwegian stations, the NOA and the ARCES array (PS27 and PS28 respectively), the radionuclide station at Spitsbergen (RN49) and the auxiliary seismic stations on Spitsbergen (AS72) and Jan Mayen (AS73) have been certified. Provided that adequate funding continues to be made available (from the CTBTO/PTS and the Norwegian Ministry of Foreign Affairs), we envisage continuing the provision of data from these and other Norwegian IMS- designated stations in accordance with current procedures. As part of NORSAR's obsolescence management, a recapitalization plan for PS27 and PS28 was submitted to CTBTO/PTS in October 2008, in order to prevent severe degradation of the stations due to lack of spare parts. The installation of new equipment will start in 2010.

The IMS infrasound station originally planned to be located near Karasjok (IS37) may need to be moved to another site, since the local authorities have not granted the permissions required for the establishment of the station. Alternative locations outside Karasjok are currently being pursued. We have identified two alternative sites in northern Norway for possible installation of IS37. The CTBTO PrepCom has approved a corresponding coordinate change for the site.

Summaries of four scientific and technical contributions presented in Chapter 6 of this report are provided below:

Section 6.1 contains results from a project aimed at improving seismic and infrasonic monitoring tools at regional distances, with emphasis on the European Arctic region, which includes the former Novaya Zemlya test site. The project has three main components: a) to improve seismic processing in this region using the regional seismic arrays installed in northern Europe, b) to investigate the potential of using combined seismic/infrasonic processing to characterize events in this region and c) to carry out experimental operation, evaluation and tuning of the seismic threshold monitoring technique.

On 11 November 2009, signals from a magnitude 3.2 event in the eastern Barents Sea were recorded by seismic stations in the Nordic countries and in NW Russia. This part of the Barents Sea has no known history of significant earthquake activity. However, over the past decades, several seismic events at various locations in this region have been detected, and several of these have been confidently associated with anthropogenic activity, like the Kursk submarine accident. As to the source type of the 11 November 2009 event, we are not in a position to draw a firm conclusion. Observations at the ARCES array, at a distance of 800 km, show signal energy up to 40 Hz and show no indication of spectral banding or cepstral peaks. This is quite different from the characteristics of underwater explosions in this area, suggesting that the event is more likely to be an earthquake. This study further illustrates the very efficient high-frequency seismic energy propagation characteristics of the Barents Sea area.

Seismic and infrasound signals at ARCES have recently been associated with blasting at the Suurikuusikko gold mine in northern Finland, approximately 10 km to the west of Hukkakero. This mine started operations in the summer of 2006 and, in order to develop a database of explosions, multi-channel waveform correlation detectors were initiated using ARCES seismic signals as templates. Many hundreds of clear detections have been made indicating several events per week. The absence of detections prior to June 2006, and the absence of detections outside of characteristic times of days, indicate a low false alarm rate. A majority of the over 500 events detected since June 2006 have been associated with infrasound detections at ARCES and at stations of the infrasound networks of Sweden, Finland, and Russia, all at regional distances from the source and with a fortuitous coverage of directions from the mine. While the events appear to be less efficient generators of infrasound than the military munitions explosions at Hukkakero, the blasts occur throughout the year and so will sample a far greater spectrum of atmospheric profiles. Examining long time-series of observations from these well-constrained sources will hopefully improve our understanding of the conditions under which infrasound is observed within and on the edge of the so-called "Zone of Silence".

International news media reported in July 2009 on an unsuccessful launch of the new Russian intercontinental Bulava missile. The missile was launched from a submarine in the White Sea on 15 July 2009, and was reported to self-destruct during the first stage of flight. The effect of another launch failure of the Bulava missile was visually observed in northern Scandinavia on 9 December 2009, in terms of strange light phenomena in the sky. This caused considerable public attention, and it was reported after some time that the phenomena were believed to originate from an engine failure and self-destruction in the third stage of a Bulava missile. Infrasound signals from both of these launches were well recorded at several infrasound arrays in the region. Array analysis followed by tracing of the estimated back-azimuths located both infrasound sources to the White Sea. During recent years, infrasound signals been observed in the Nordic region from several rocket launches and meteors entering the atmosphere. Establishing a database of such events is important for future studies of infrasound wave propagation.

Section 6.2 is entitled: “Detecting the DPRK nuclear test explosion on 25 May 2009 using array-based waveform correlation”. The Democratic People’s Republic of Korea (DPRK) announced on 25 May 2009 that it has conducted its second nuclear test, the first one having taken place on 9 October 2006. As was the case with the first test, the second test was detected and reported by the IDC. We have in this study demonstrated that performing multi-channel cross-correlation on the MJAR array in Japan, with a signal template taken from the October 9, 2006, North Korea nuclear test, is able to detect the signals from the May 25, 2009, North

Korea test with a very low false alarm rate. Crucial to the low false alarm rate in this study is the performing of f-k analysis on the individual sensor detection statistic traces which eliminates false alarms both due to unrelated seismic signals and problems in the data.

A scaling study, whereby signals from both 2006 and 2009 tests are scaled down and submerged into the background noise, suggests that, at a detection threshold which results in a negligible number of detections, events down to magnitude ~3.0 at the site of the 2009 test are detected by the correlation procedure in 95% of cases.

It is pointed out that this study used only data from the MJAR array (Matsushiro, Japan) which, due to problems of signal incoherence at high frequencies, was unable to contribute to the automatic event location estimate for either 2006 or 2009 DPRK nuclear tests. The multi-channel correlation procedure demonstrated here is insensitive to waveform incoherence between sensors and can be used to detect signals from new events if we have a template signal from an event close-by. This is the case fothe DPRK test site and many other sources of both natural and anthropogenic seismicity. Large scale correlation detectors in operational pipelines are to be advocated for automatic signal detection and event classification.

Section 6.3 is entitled "A probabilistic seismic model for the European Arctic". The area of interest for this study includes the Barents Sea and surrounding regions such as the Norwegian-Greenland Sea, the Southern Eurasian Basin, Novaya Zemlya, the Kara Sea, the East European Lowlands, the Kola Peninsula and the Arctic plate boundary. When developing a seismic model the focus is often on finding one single best fitting model. Existing models for the region are based on approaches that try to find the model with the best fit to one or several dataset. The resulting models contain little to no information about model uncertainties. Knowledge about the robustness of features in seismic models is however beneficial for the geological interpretation of models and the reliable determination of location uncertainties for seismic events.

The probabilistic model used in this study differs from traditional seismic models in that it describes the posterior distribution, the ensemble of models which fit the data. The posterior distribution is proportional to the product of the prior distribution and the likelihood function. The prior distribution represents the ensemble of plausible models and the likelihood function makes models with a good fit to the data more likely than models with bad fit to the data. The data used are thickness constraints, velocity profiles, gravity data, surface wave group velocities and body wave travel times. In this work a Markov Chain Monte Carlo (MCMC) technique is used to sample the unknown posterior distribution. This process results in 4,000 models that all fit the data. Analyzing this ensemble of models that fit the data allows estimating a mean model and the standard deviation for the model parameters, i.e. their uncertainty. Maps of sediment thickness and thickness of the crystalline crust derived from the posterior distribution are in good agreement with knowledge of the regional tectonic setting. The predicted uncertainties, which are equally important as the absolute values, correlate well with the variation in data coverage and data quality in the region. In addition to this a probabilistic model allows the formulation of seismic event location techniques that take into account uncertainties in the velocity model.

In conclusion, this study has successfully employed a probabilistic approach for the development of a data-driven regional seismic model for the European Arctic. The mean model of our posterior distribution has been compared with other models that cover the region and fit has been found that it captures the features that can be resolved with a node spacing of 83 km. The probabilistic model not only provides images of the subsurface together with estimates of

uncertainties, it also allows for the prediction of observables and uncertainties. This can be used to derive seismic event location uncertainties from model uncertainties and can in the future be used for location algorithms that take model uncertainties in addition to uncertainties in onset time into account.

Section 6.4 is entitled: "Local seismicity on and near Bear Island (Norwegian Arctic) from a temporary small aperture array installation in 2008". This installation was part of the International Polar Year project "The dynamic continental margin between the Mid Atlantic-Ridge system (Mohns Ridge, Knipovich Ridge) and the Bear Island region". The aim of this project was to improve the understanding of the structural architecture, the stress conditions and sources, the dynamics of the continental margin, and to identify active tectonic structures. Using this array together with 12 ocean bottom seismometers and two new broadband seismometers on Svalbard and Hopen a large number of earthquakes could be detected along the Mohns and Knipovich ridge and the Senja Fracture Zone as well as a magnitude 6 earthquake near Svalbard in February 2008 with a large number of aftershocks.

However, the vast majority of the seismic events recorded by the Bear Island array are clearly of local origin. These local events seem to have different sources. They could be due to human activity at the meteorological station in the northern part of Bear Island, but could also be caused by weather and climate phenomena, the melting of snow or the drifting and breaking of ice floes on the rivers and lakes on Bear Island. Rockfall along the steep coastal line or at the mountainous southern part of the island would be another plausible explanation. Of greatest interest are a number of presumably tectonic events on or near the island, southeast of the array. These events are still under investigation.

Frode Ringdal

AFTAC Project Authorization	:	T/6110
Purchase Request No.	:	F3KTK85290A1
Name of Contractor	:	Stiftelsen NORSAR
Effective Date of Contract	:	1 March 2006
Contract Expiration Date	:	30 September 2011
Amount of Contract	:	$ 1,003,494.00
Project Manager	:	Frode Ringdal +47 63 80 59 00
Title of Work	:	The Norwegian Seismic Array (NORSAR) Phase 3
Period Covered by Report	:	1 January - 30 June 2010

The views and conclusions contained in this document are those of the authors and should not be interpreted as necessarily representing the official policies, either expressed or implied, of the U.S. Government.

Part of the research presented in this report was supported by the Army Space and Missile Defense Command, under contract no. W9113M-05-C-0224. Other activities were supported and monitored by AFTAC, Patrick AFB, FL32925, under contract no. FA2521-06-C-8003. Other sponsors are acknowledged where appropriate.

The operational activities of the seismic field systems and the Norwegian National Data Center (NDC) are currently jointly funded by the Norwegian Government and the CTBTO/PTS, with the understanding that the funding of appropriate IMS-related activities will gradually be transferred to the CTBTO/PTS.

Table of Contents

Page

1 Summary

This report describes activities carried out at NORSAR under Contract No. FA2521-06-C-8003 for the period 1 January - 30 June 2010. In addition, it provides summary information on operation and maintenance (O&M) activities at the Norwegian National Data Center (NOR- NDC) during the same period. The O&M activities, including operation of transmission links within Norway and to Vienna, Austria are being funded jointly by the CTBTO/PTS and the Norwegian Government, with the understanding that the funding of O&M activities for primary stations in the International Monitoring System (IMS) will gradually be transferred to the CTBTO/PTS. The O&M statistics presented in this report are included for the purpose of completeness, and in order to maintain consistency with earlier reporting practice. Some of the research activities described in this report are funded by the United States Government, and the United States also covers the cost of transmission of selected data from the Norwegian NDC to the United States NDC.

The seismic arrays operated by NOR-NDC comprise the Norwegian Seismic Array (NOA), the Arctic Regional Seismic Array (ARCES) and the Spitsbergen Regional Array (SPITS). This report presents statistics for these three arrays as well as for additional seismic stations which through cooperative agreements with institutions in the host countries provide continuous data to NOR-NDC. These additional stations include the Finnish Regional Seismic Array (FINES) and the Hagfors array in Sweden (HFS).

The NOA Detection Processing system has been operated throughout the period with an uptime of 100%. A total of 2,087 seismic events have been reported in the NOA monthly seismic bulletin during the reporting period. On-line detection processing and data recording at the NDC of data from ARCES, FINES, SPITS and HFS data have been conducted throughout the period. Processing statistics for the arrays for the reporting period are given.

A summary of the activities at the NOR-NDC and relating to field installations during the reporting period is provided in Section 4. Norway is now contributing primary station data from two seismic arrays: NOA (PS27) and ARCES (PS28), one auxiliary seismic array SPITS (AS72), and one auxiliary three-component station JMIC (AS73). These data are being provided to the IDC via the global communications infrastructure (GCI). Continuous data from the three arrays are in addition being transmitted to the US NDC. The performance of the data transmission to the US NDC has been satisfactory during the reporting period.

So far among the Norwegian stations, the NOA and the ARCES array (PS27 and PS28 respectively), the radionuclide station at Spitsbergen (RN49) and the auxiliary seismic stations on Spitsbergen (AS72) and Jan Mayen (AS73) have been certified. Provided that adequate funding continues to be made available (from the CTBTO/PTS and the Norwegian Ministry of Foreign Affairs), we envisage continuing the provision of data from these and other Norwegian IMS- designated stations in accordance with current procedures. As part of NORSAR's obsolescence management, a recapitalization plan for PS27 and PS28 was submitted to CTBTO/PTS in October 2008, in order to prevent severe degradation of the stations due to lack of spare parts. The installation of new equipment will start in 2010.

The IMS infrasound station originally planned to be located near Karasjok (IS37) may need to be moved to another site, since the local authorities have not granted the permissions required for the establishment of the station. Alternative locations outside Karasjok are currently being pursued. We have identified two alternative sites in northern Norway for possible installation of IS37. The CTBTO PrepCom has approved a corresponding coordinate change for the site.

Summaries of four scientific and technical contributions presented in Chapter 6 of this report are provided below:

Section 6.1 contains results from a project aimed at improving seismic and infrasonic monitoring tools at regional distances, with emphasis on the European Arctic region, which includes the former Novaya Zemlya test site. The project has three main components: a) to improve seismic processing in this region using the regional seismic arrays installed in northern Europe, b) to investigate the potential of using combined seismic/infrasonic processing to characterize events in this region and c) to carry out experimental operation, evaluation and tuning of the seismic threshold monitoring technique.

On 11 November 2009, signals from a magnitude 3.2 event in the eastern Barents Sea were recorded by seismic stations in the Nordic countries and in NW Russia. This part of the Barents Sea has no known history of significant earthquake activity. However, over the past decades, several seismic events at various locations in this region have been detected, and several of these have been confidently associated with anthropogenic activity, like the Kursk submarine accident. As to the source type of the 11 November 2009 event, we are not in a position to draw a firm conclusion. Observations at the ARCES array, at a distance of 800 km, show signal energy up to 40 Hz and show no indication of spectral banding or cepstral peaks. This is quite different from the characteristics of underwater explosions in this area, suggesting that the event is more likely to be an earthquake. This study further illustrates the very efficient high-frequency seismic energy propagation characteristics of the Barents Sea area.

Seismic and infrasound signals at ARCES have recently been associated with blasting at the Suurikuusikko gold mine in northern Finland, approximately 10 km to the west of Hukkakero. This mine started operations in the summer of 2006 and, in order to develop a database of explosions, multi-channel waveform correlation detectors were initiated using ARCES seismic signals as templates. Many hundreds of clear detections have been made indicating several events per week. The absence of detections prior to June 2006, and the absence of detections outside of characteristic times of days, indicate a low false alarm rate. A majority of the over 500 events detected since June 2006 have been associated with infrasound detections at ARCES and at stations of the infrasound networks of Sweden, Finland, and Russia, all at regional distances from the source and with a fortuitous coverage of directions from the mine. While the events appear to be less efficient generators of infrasound than the military munitions explosions at Hukkakero, the blasts occur throughout the year and so will sample a far greater spectrum of atmospheric profiles. Examining long time-series of observations from these well-constrained sources will hopefully improve our understanding of the conditions under which infrasound is observed within and on the edge of the so-called "Zone of Silence".

International news media reported in July 2009 on an unsuccessful launch of the new Russian intercontinental Bulava missile. The missile was launched from a submarine in the White Sea on 15 July 2009, and was reported to self-destruct during the first stage of flight. The effect of another launch failure of the Bulava missile was visually observed in northern Scandinavia on 9 December 2009, in terms of strange light phenomena in the sky. This caused considerable public attention, and it was reported after some time that the phenomena were believed to originate from an engine failure and self-destruction in the third stage of a Bulava missile. Infrasound signals from both of these launches were well recorded at several infrasound arrays in the region. Array analysis followed by tracing of the estimated back-azimuths located both infrasound sources to the White Sea. During recent years, infrasound signals been observed in the Nordic region from several rocket launches and meteors entering the atmosphere. Estab-

lishing a database of such events is important for future studies of infrasound wave propagation.

Section 6.2 is entitled: "Detecting the DPRK nuclear test explosion on 25 May 2009 using array-based waveform correlation". The Democratic People's Republic of Korea (DPRK) announced on 25 May 2009 that it has conducted its second nuclear test, the first one having taken place on 9 October 2006. As was the case with the first test, the second test was detected and reported by the IDC. We have in this study demonstrated that performing multi-channel cross-correlation on the MJAR array in Japan, with a signal template taken from the October 9, 2006, North Korea nuclear test, is able to detect the signals from the May 25, 2009, North Korea test with a very low false alarm rate. Crucial to the low false alarm rate in this study is the performing of f-k analysis on the individual sensor detection statistic traces which eliminates false alarms both due to unrelated seismic signals and problems in the data.

A scaling study, whereby signals from both 2006 and 2009 tests are scaled down and submerged into the background noise, suggests that, at a detection threshold which results in a negligible number of detections, events down to magnitude ~3.0 at the site of the 2009 test are detected by the correlation procedure in 95% of cases.

It is pointed out that this study used only data from the MJAR array (Matsushiro, Japan) which, due to problems of signal incoherence at high frequencies, was unable to contribute to the automatic event location estimate for either 2006 or 2009 DPRK nuclear tests. The multi-channel correlation procedure demonstrated here is insensitive to waveform incoherence between sensors and can be used to detect signals from new events if we have a template signal from an event close-by. This is the case fothe DPRK test site and many other sources of both natural and anthropogenic seismicity. Large scale correlation detectors in operational pipelines are to be advocated for automatic signal detection and event classification.

Section 6.3 is entitled "A probabilistic seismic model for the European Arctic". The area of interest for this study includes the Barents Sea and surrounding regions such as the Norwegian-Greenland Sea, the Southern Eurasian Basin, Novaya Zemlya, the Kara Sea, the East European Lowlands, the Kola Peninsula and the Arctic plate boundary. When developing a seismic model the focus is often on finding one single best fitting model. Existing models for the region are based on approaches that try to find the model with the best fit to one or several dataset. The resulting models contain little to no information about model uncertainties. Knowledge about the robustness of features in seismic models is however beneficial for the geological interpretation of models and the reliable determination of location uncertainties for seismic events.

The probabilistic model used in this study differs from traditional seismic models in that it describes the posterior distribution, the ensemble of models which fit the data. The posterior distribution is proportional to the product of the prior distribution and the likelihood function. The prior distribution represents the ensemble of plausible models and the likelihood function makes models with a good fit to the data more likely than models with bad fit to the data. The data used are thickness constraints, velocity profiles, gravity data, surface wave group velocities and body wave travel times. In this work a Markov Chain Monte Carlo (MCMC) technique is used to sample the unknown posterior distribution. This process results in 4,000 models that all fit the data. Analyzing this ensemble of models that fit the data allows estimating a mean model and the standard deviation for the model parameters, i.e. their uncertainty. Maps of sediment thickness and thickness of the crystalline crust derived from the posterior distribution are in good agreement with knowledge of the regional tectonic setting. The predicted uncertainties,

which are equally important as the absolute values, correlate well with the variation in data coverage and data quality in the region. In addition to this a probabilistic model allows the formulation of seismic event location techniques that take into account uncertainties in the velocity model.

In conclusion, this study has successfully employed a probabilistic approach for the development of a data-driven regional seismic model for the European Arctic. The mean model of our posterior distribution has been compared with other models that cover the region and fit has been found that it captures the features that can be resolved with a node spacing of 83 km. The probabilistic model not only provides images of the subsurface together with estimates of uncertainties, it also allows for the prediction of observables and uncertainties. This can be used to derive seismic event location uncertainties from model uncertainties and can in the future be used for location algorithms that take model uncertainties in addition to uncertainties in onset time into account.

Section 6.4 is entitled: "Local seismicity on and near Bear Island (Norwegian Arctic) from a temporary small aperture array installation in 2008". This installation was part of the International Polar Year project "The dynamic continental margin between the Mid Atlantic-Ridge system (Mohns Ridge, Knipovich Ridge) and the Bear Island region". The aim of this project was to improve the understanding of the structural architecture, the stress conditions and sources, the dynamics of the continental margin, and to identify active tectonic structures. Using this array together with 12 ocean bottom seismometers and two new broadband seismometers on Svalbard and Hopen a large number of earthquakes could be detected along the Mohns and Knipovich ridge and the Senja Fracture Zone as well as a magnitude 6 earthquake near Svalbard in February 2008 with a large number of aftershocks.

However, the vast majority of the seismic events recorded by the Bear Island array are clearly of local origin. These local events seem to have different sources. They could be due to human activity at the meteorological station in the northern part of Bear Island, but could also be caused by weather and climate phenomena, the melting of snow or the drifting and breaking of ice floes on the rivers and lakes on Bear Island. Rockfall along the steep coastal line or at the mountainous southern part of the island would be another plausible explanation. Of greatest interest are a number of presumably tectonic events on or near the island, southeast of the array. These events are still under investigation.

Frode Ringdal

2 Operation of International Monitoring System (IMS) Stations in Norway

2.1 PS27 — Primary Seismic Station NOA

The mission-capable data statistics were 100%, the same as for the previous reporting period. The net instrument availability was 98.160%.

There were no outages of all subarrays at the same time in the reporting period.

Monthly uptimes for the NORSAR on-line data recording task, taking into account all factors (field installations, transmissions line, data center operation) affecting this task were as follows:

2010		Mission Capable	Net instrument availability
January	:	100%	97.781%
February	:	100%	98.161%
March	:	100%	98.361%
April	:	100%	98.408%
May	:	100%	97.859%
June	:	100%	98.403%

B. Paulsen

NOA Event Detection Operation

In Table 2.1.1 some monthly statistics of the Detection and Event Processor operation are given. The table lists the total number of detections (DPX) triggered by the on-line detector, the total number of detections processed by the automatic event processor (EPX) and the total number of events accepted after analyst review (teleseismic phases, core phases and total).

	Total DPX	Total EPX	Accepted Events		Sum	Daily
			P-phases	Core Phases		
Jan	12,080	1,017	299	68	367	11.8
Feb	9,903	891	258	80	338	12.1
Mar	11,465	1,013	269	82	351	11.3
Apr	9,904	952	277	79	356	11.9
May	6,079	860	262	72	334	10.8
Jun	7,324	1,104	280	61	341	11.4
	56,755	5,837	1,645	442	2,087	11.5

Table 2.1.1. *Detection and Event Processor statistics, 1 January - 30 June 2010.*

NOA detections

The number of detections (phases) reported by the NORSAR detector during day 001, 2010, through day 181, 2010, was 56,755, giving an average of 314 detections per processed day (181 days processed).

B. Paulsen
U. Baadshaug

2.2 PS28 — Primary Seismic Station ARCES

The mission-capable data statistics were 99.997%, as compared to 100% for the previous reporting period. The net instrument availability was 99.536%.

The main outages in the period are presented in Table 2.2.1.

Day	Period
28 Jan	11.47-11.48
05 May	13.19-13.21
15 Jun	08.10-08.11

Table 2.2.1. *The main interruptions in recording of ARCES data at NDPC, 1 January - 30 June 2010.*

Monthly uptimes for the ARCES on-line data recording task, taking into account all factors (field installations, transmission lines, data center operation) affecting this task were as follows:

2010		Mission Capable	Net instrument availability
January	:	99.993%	99.349%
February	:	100%	98.817%
March	:	100%	99.146%
April	:	100%	99.871%
May	:	99.996%	99.996%
June	:	99.997%	99.996%

B. Paulsen

Event Detection Operation

ARCES detections

The number of detections (phases) reported during day 001, 2010, through day 181, 2010, was 191,650, giving an average of 1059 detections per processed day (181 days processed).

Events automatically located by ARCES

During days 001, 2010, through 181, 2010, 10,231 local and regional events were located by ARCES, based on automatic association of P- and S-type arrivals. This gives an average of 56.5 events per processed day (181 days processed). 75% of these events are within 300 km, and 92 % of these events are within 1000 km.

U. Baadshaug

2.3 AS72 — Auxiliary Seismic Station Spitsbergen

The mission-capable data for the period were 98.001%, as compared to 99.226% for the previous reporting period. The net instrument availability was 92.878%.

The main outages in the period are presented in Table 2.3.1.

Day	Period
04 Jan	12.16-00.00
05 Jan	00.00-24.00
06 Jan	00.00-24.00
25 Jan	13.08-13.23
06 Apr	10.58-24.00
07 Apr	00.00-12.37
30 Apr	07.53-08.34

Table 2.3.1. *The main interruptions in recording of Spitsbergen data at NDPC, 1 January - 30 June 2010. Data during the outage periods have been back-filled.*

Monthly uptimes for the Spitsbergen on-line data recording task, taking into account all factors (field installations, transmissions line, data center operation) affecting this task were as follows:

2010		Mission Capable	Net instrument availability
January	:	91.932%	75.606%
February	:	100%	98.817%
March	:	99.991%	95.229%
April	:	96.333%	91.821%
May	:	99.997%	99.926%
June	:	99.962%	99.871%

B. Paulsen

Event Detection Operation

Spitsbergen array detections

The number of detections (phases) reported from day 001, 2010, through day 181, 2010, was 378,088, giving an average of 2,089 detections per processed day (181 days processed).

Events automatically located by the Spitsbergen array

During days 001, 2010 through 181, 2010, 29,985 local and regional events were located by the Spitsbergen array, based on automatic association of P- and S-type arrivals. This gives an average of 165.7 events per processed day (181 days processed). 75% of these events are within 300 km, and 91% of these events are within 1000 km.

U. Baadshaug

2.4 AS73 — Auxiliary Seismic Station at Jan Mayen

The IMS auxiliary seismic network includes a three-component station on the Norwegian island of Jan Mayen. The station location given in the protocol to the Comprehensive Nuclear-Test-Ban Treaty is 70.9°N, 8.7°W.

The University of Bergen has operated a seismic station at this location since 1970. A so-called Parent Network Station Assessment for AS73 was completed in April 2002. A vault at a new location (71.0^{o}N, 8.5^{o}W) was prepared in early 2003, after its location had been approved by the PrepCom. New equipment was installed in this vault in October 2003, as a cooperative effort between NORSAR and the CTBTO/PTS. Continuous data from this station are being transmitted to the NDC at Kjeller via a satellite link installed in April 2000. Data are also made available to the University of Bergen.

The station was certified by the CTBTO/PTS on 12 June 2006.

J. Fyen

2.5 IS37 — Infrasound Station at Karasjok

The IMS infrasound network will, according to the protocol of the CTBT, include a station at Karasjok in northern Norway. The coordinates given for this station are 69.5°N, 25.5°E. These coordinates coincide with those of the primary seismic station PS28.

It has, however, proved very difficult to obtain the necessary permits for use of land for an infrasound station in Karasjok. Various alternatives for locating the station in Karasjok were prepared, but all applications to the local authorities to obtain the permissions needed to establish the station were turned down by the local governing council in June 2007.

In 2008, investigations were initiated to identify an alternative site for IS37 outside Karasjok. Two sites at Bardufoss, at 69.1^{o} N, 18.6^{o} E, are currently being pursued with landowners and the municipal authorities, with the purpose of selecting one of them for possible installation of IS37. The CTBTO PrepCom has approved a corresponding coordinate change for the station.

J. Fyen

2.6 RN49 — Radionuclide Station on Spitsbergen

The IMS radionuclide network includes a station on the island of Spitsbergen. This station has been selected to be among those IMS radionuclide stations that will monitor for the presence of relevant noble gases upon entry into force of the CTBT.

A site survey for this station was carried out in August of 1999 by NORSAR, in cooperation with the Norwegian Radiation Protection Authority. The site survey report to the PTS contained a recommendation to establish this station at Platåberget, near Longyearbyen. The infrastructure for housing the station equipment was established in early 2001, and a noble gas detection system, based on the Swedish "SAUNA" design, was installed at this site in May 2001, as part of PrepCom's noble gas experiment. A particulate station ("ARAME" design) was installed at the same location in September 2001. A certification visit to the particulate station took place in October 2002, and the particulate station was certified on 10 June 2003. Both systems underwent substantial upgrading in May/June 2006. The equipment at RN49 is being maintained and operated under a contract with the CTBTO/PTS.

S. Mykkeltveit

3 Contributing Regional Seismic Arrays

3.1 NORES

NORES has been out of operation since lightning destroyed the station electronics on 11 June 2002.

B. Paulsen

3.2 Hagfors (IMS Station AS101)

Data from the Hagfors array are made available continuously to NORSAR through a cooperative agreement with Swedish authorities.

The mission-capable data statistics were 99.999%, as compared to 99.982% for the previous reporting period. The net instrument availability was 99.999%.

The were no outages in the period.

Monthly uptimes for the Hagfors on-line data recording task, taking into account all factors (field installations, transmissions line, data center operation) affecting this task were as follows:

2010		Mission Capable	Net instrument availability
January	:	100%	100%
February	:	100%	100%
March	:	100%	100%
April	:	99.997%	99.997%
May	:	100%	100%
June	:	100%	100%

B. Paulsen

Hagfors Event Detection Operation

Hagfors array detections

The number of detections (phases) reported from day 001, 2010, through day 181, 2010, was 137,773, giving an average of 761 detections per processed day (181 days processed).

Events automatically located by the Hagfors array

During days 001, 2010, through 181, 2010, 4,169 local and regional events were located by the Hagfors array, based on automatic association of P- and S-type arrivals. This gives an average of 23.0 events per processed day (181 days processed). 74% of these events are within 300 km, and 93% of these events are within 1000 km.

U. Baadshaug

3.3 FINES (IMS station PS17)

Data from the FINES array are made available continuously to NORSAR through a cooperative agreement with Finnish authorities.

The mission-capable data statistics were 94.662%, as compared to 97.738% for the previous reporting period. The net instrument availability was 92.688%.

The main outages in the period are presented in Table 3.3.1.

Day	Period
28 Jan	06.29-12.35
03 Feb	03.49-10.26
19 Feb	11.06-24.00
20 Feb	00.00-24.00
21 Feb	00.00-24.00
26 Apr	09.45-24.00
27 Apr	00.00-24.00
28 Apr	00.00-24.00
29 Apr	00.00-24.00
30 Apr	00.00-24.00
01 May	00.00-24.00
02 May	00.00-24.00

Table 3.3.1. *The main interruptions in recording of FINES data at NDPC, 1 January - 30 June 2010. Data during the outage periods have been back-filled.*

Monthly uptimes for the FINES on-line data recording task, taking into account all factors (field installations, transmissions line, data center operation) affecting this task were as follows:

2010		Mission Capable	Net instrument availability
January	:	99.180%	98.754%
February	:	89.954%	88.880%
March	:	100%	96.226%
April	:	84.687%	80.654%
May	:	93.548%	91.091%
June	:	100%	100%

B. Paulsen

FINES Event Detection Operation

FINES detections

The number of detections (phases) reported during day 001, 2010, through day 181, 2010, was 38,839, giving an average of 215 detections per processed day (181 days processed).

Events automatically located by FINES

During days 001, 2010, through 181, 2010, 2,211 local and regional events were located by FINES, based on automatic association of P- and S-type arrivals. This gives an average of 12.2 events per processed day (181 days processed). 87% of these events are within 300 km, and 94% of these events are within 1000 km.

U. Baadshaug

3.4 Regional Monitoring System Operation and Analysis

The Regional Monitoring System (RMS) was installed at NORSAR in December 1989 and has been operated at NORSAR from 1 January 1990 for automatic processing of data from ARCES and NORES. A second version of RMS that accepts data from an arbitrary number of arrays and single 3-component stations was installed at NORSAR in October 1991, and regular operation of the system comprising analysis of data from the 4 arrays ARCES, NORES, FINES and GERES started on 15 October 1991. As opposed to the first version of RMS, the one in current operation also has the capability of locating events at teleseismic distances.

Data from the Apatity array was included on 14 December 1992, and from the Spitsbergen array on 12 January 1994. Detections from the Hagfors array were available to the analysts and could be added manually during analysis from 6 December 1994. After 2 February 1995, Hagfors detections were also used in the automatic phase association.

Since 24 April 1999, RMS has processed data from all the seven regional arrays ARCES, NORES, FINES, GERES (until January 2000), Apatity, Spitsbergen, and Hagfors. Starting 19 September 1999, waveforms and detections from the NORSAR array have also been available to the analyst.

Phase and event statistics

Table 3.5.1 gives a summary of phase detections and events declared by RMS. From top to bottom the table gives the total number of detections by the RMS, the number of detections that are associated with events automatically declared by the RMS, the number of detections that are not associated with any events, the number of events automatically declared by the RMS, and finally the total number of events worked on interactively (in accordance with criteria that vary over time; see below) and defined by the analyst.

New criteria for interactive event analysis were introduced from 1 January 1994. Since that date, only regional events in areas of special interest (e.g, Spitsbergen, since it is necessary to acquire new knowledge in this region) or other significant events (e.g, felt earthquakes and large industrial explosions) were thoroughly analyzed. Teleseismic events of special interest are also analyzed.

To further reduce the workload on the analysts and to focus on regional events in preparation for Gamma-data submission during GSETT-3, a new processing scheme was introduced on 2

February 1995. The GBF (Generalized Beamforming) program is used as a pre-processor to RMS, and only phases associated with selected events in northern Europe are considered in the automatic RMS phase association. All detections, however, are still available to the analysts and can be added manually during analysis.

	Jan 10	Feb 10	Mar 10	Apr 10	May 10	Jun 10	Total
Phase detections	147,930	147,412	152,054	137,002	137,374	118,260	840,032
- Associated phases	4,241	5,372	5,942	5,967	5,827	5,437	32,786
- Unassociated phases	143,689	142,040	146,112	131,035	131,547	112,823	807,246
Events automatically declared by RMS	857	985	1,132	1,010	1,045	1,082	6,111
No. of events defined by the analyst	47	80	76	84	81	89	457

Table 3.5.1. RMS phase detections and event summary 1 January - 30 June 2010.

U. Baadshaug

B. Paulsen

4 NDC and Field Activities

4.1 NDC Activitities

NORSAR functions as the Norwegian National Data Center (NDC) for CTBT verification. Six monitoring stations, comprising altogether 132 field sensors plus radionuclide monitoring equipment, will be located on Norwegian territory as part of the future IMS as described elsewhere in this report. The four seismic IMS stations are all in operation today, and all of them are currently providing data to the CTBTO on a regular basis. PS27, PS28, AS72, AS73 and RN49 are all certified. Data recorded by the Norwegian stations is being transmitted in real time to the Norwegian NDC, and provided to the IDC through the Global Communications Infrastructure (GCI). Norway is connected to the GCI with a frame relay link to Vienna.

Operating the Norwegian IMS stations continues to require significant efforts by personnel both at the NDC and in the field. Strictly defined procedures as well as increased emphasis on regularity of data recording and timely data transmission to the IDC in Vienna have led to increased reporting activities and implementation of new procedures for the NDC. The NDC carries out all the technical tasks required in support of Norway's treaty obligations. NORSAR will also carry out assessments of events of special interest, and advise the Norwegian authorities in technical matters relating to treaty compliance. A challenge for the NDC is to carry 40 years' experience over to the next generation of personnel.

Verification functions; information received from the IDC

After the CTBT enters into force, the IDC will provide data for a large number of events each day, but will not assess whether any of them are likely to be nuclear explosions. Such assessments will be the task of the States Parties, and it is important to develop the necessary national expertise in the participating countries. An important task for the Norwegian NDC will thus be to make independent assessments of events of particular interest to Norway, and to communicate the results of these analyses to the Norwegian Ministry of Foreign Affairs.

Monitoring the Arctic region

Norway will have monitoring stations of key importance for covering the Arctic, including Novaya Zemlya, and Norwegian experts have a unique competence in assessing events in this region. On several occasions in the past, seismic events near Novaya Zemlya have caused political concern, and NORSAR specialists have contributed to clarifying these issues.

International cooperation

After entry into force of the treaty, a number of countries are expected to establish national expertise to contribute to the treaty verification on a global basis. Norwegian experts have been in contact with experts from several countries with the aim of establishing bilateral or multilateral cooperation in this field. One interesting possibility for the future is to establish NORSAR as a regional center for European cooperation in the CTBT verification activities.

NORSAR event processing

The automatic routine processing of NORSAR events as described in NORSAR Sci. Rep. No. 2-93/94, has been running satisfactorily. The analyst tools for reviewing and updating the solu-

tions have been continually modified to simplify operations and improve results. NORSAR is currently applying teleseismic detection and event processing using the large-aperture NOA array as well as regional monitoring using the network of small-aperture arrays in Fennoscandia and adjacent areas.

Communication topology

Norway has implemented an independent subnetwork, which connects the IMS stations AS72, AS73, PS28, and RN49 operated by NORSAR to the GCI at NOR_NDC. A contract has been concluded and VSAT antennas have been installed at each station in the network. Under the same contract, VSAT antennas for 6 of the PS27 subarrays have been installed for intra-array communication. The seventh subarray is connected to the central recording facility via a leased land line. The central recording facility for PS27 is connected directly to the GCI (Basic Topology). All the VSAT communication is functioning satisfactorily. As of 10 June 2005, AS72 and RN49 are connected to NOR_NDC through a VPN link.

Jan Fyen

4.2 Status Report: Provision of data from Norwegian seismic IMS stations to the IDC

Introduction

This contribution is a report for the period January - June 2010 on activities associated with provision of data from Norwegian seismic IMS stations to the International Data Centre (IDC) in Vienna. This report represents an update of contributions that can be found in previous editions of NORSAR's Semiannual Technical Summary. All four Norwegian seismic stations providing data to the IDC have now been formally certified.

Norwegian IMS stations and communications arrangements

During the reporting interval, Norway has provided data to the IDC from the four seismic stations shown in Fig. 4.2.1. PS27 —NOA is a 60 km aperture teleseismic array, comprised of 7 subarrays, each containing six vertical short period sensors and a three-component broadband instrument. PS28 — ARCES is a 25-element regional array with an aperture of 3 km, whereas AS72 — Spitsbergen array (station code SPITS) has 9 elements within a 1-km aperture. AS73 — JMIC has a single three-component broadband instrument.

The intra-array communication for NOA utilizes a land line for subarray NC6 and VSAT links based on TDMA technology for the other 6 subarrays. The central recording facility for NOA is located at the Norwegian National Data Center (NOR_NDC).

Continuous ARCES data are transmitted from the ARCES site to NOR_NDC using a 64 kbits/s VSAT satellite link, based on BOD technology.

Continuous SPITS data were transmitted to NOR_NDC via a VSAT terminal located at Platåberget in Longyearbyen (which is the site of the IMS radionuclide monitoring station RN49 installed during 2001) up to 10 June 2005. The central recording facility (CRF) for the SPITS array has been moved to the University of Spitsbergen (UNIS). A 512 bps SHDSL link has been established between UNIS and NOR_NDC. Data from the array elements to the CRF are

transmitted via a 2.4 Ghz radio link (Wilan VIP-110). Both AS72 and RN49 data are now transmitted to NOR_NDC over this link using VPN technology.

A minimum of seven-day station buffers have been established at the ARCES and SPITS sites and at all NOA subarray sites, as well as at the NOR_NDC for ARCES, SPITS and NOA. In addition, each individual site of the SPITS array has a 14-day buffer.

The NOA and ARCES arrays are primary stations in the IMS network, which implies that data from these stations is transmitted continuously to the receiving international data center. Since October 1999, this data has been transmitted (from NOR_NDC) via the Global Communications Infrastructure (GCI) to the IDC in Vienna. Data from the auxiliary array station SPITS — AS72 have been sent in continuous mode to the IDC during the reporting period. AS73 — JMIC is an auxiliary station in the IMS, and the JMIC data have been available to the IDC throughout the reporting period on a request basis via use of the AutoDRM protocol (Kradolfer, 1993; Kradolfer, 1996). In addition, continuous data from all three arrays is transmitted to the US_NDC.

Uptimes and data availability

Figs. 4.2.2 and 4.2.3 show the monthly uptimes for the Norwegian IMS primary stations ARCES and NOA, respectively, for the reporting period given as the hatched (taller) bars in these figures. These barplots reflect the percentage of the waveform data that is available in the NOR_NDC data archives for these two arrays. The downtimes inferred from these figures thus represent the cumulative effect of field equipment outages, station site to NOR_NDC communication outage, and NOR_NDC data acquisition outages.

Figs. 4.2.2 and 4.2.3 also give the data availability for these two stations as reported by the IDC in the IDC Station Status reports. The main reason for the discrepancies between the NOR_NDC and IDC data availabilities as observed from these figures is the difference in the ways the two data centers report data availability for arrays: Whereas NOR_NDC reports an array station to be up and available if at least one channel produces useful data, the IDC uses weights where the reported availability (capability) is based on the number of actually operating channels.

Use of the AutoDRM protocol

NOR_NDC's AutoDRM has been operational since November 1995 (Mykkeltveit & Baadshaug, 1996). The monthly number of requests by the IDC for JMIC data for the period January - June 2010 is shown in Fig. 4.2.4.

NDC automatic processing and data analysis

These tasks have proceeded in accordance with the descriptions given in Mykkeltveit and Baadshaug (1996). For the reporting period NOR_NDC derived information on 458 supplementary events in northern Europe and submitted this information to the Finnish NDC as the NOR_NDC contribution to the joint Nordic Supplementary (Gamma) Bulletin, which in turn is forwarded to the IDC. These events are plotted in Fig. 4.2.5.

Data access for the station NIL at Nilore, Pakistan

NOR_NDC has for many years provided access to the seismic station NIL at Nilore, Pakistan, through a VSAT satellite link between NOR_NDC and Nilore. In late July 2009, the VSAT ground station equipment at Nilore failed, and it turned out that this equipment is obsolete and cannot be repaired. The service provider has proposed the installation of new equipment. Following some technical clarifications, NORSAR will submit to AFTAC a proposal for a new satellite communications system between NOR_NDC and Nilore.

Current developments and future plans

NOR_NDC is continuing the efforts towards improving and hardening all critical data acquisition and data forwarding hardware and software components, so as to meet the requirements related to operation of IMS stations.

The NOA array was formally certified by the PTS on 28 July 2000, and a contract with the PTS in Vienna currently provides partial funding for operation and maintenance of this station. The ARCES array was formally certified by the PTS on 8 November 2001, and a contract with the PTS is in place which also provides for partial funding of the operation and maintenance of this station. The operation of the two IMS auxiliary seismic stations on Norwegian territory (Spitsbergen and Jan Mayen) is funded by the Norwegian Ministry of Foreign Affairs. Provided that adequate funding continues to be made available (from the PTS and the Norwegian Ministry of Foreign Affairs), we envisage continuing the provision of data from all Norwegian seismic IMS stations without interruption to the IDC in Vienna.

The two stations PS27 and PS28 are both suffering from lack of spare parts. The PS27 NOA equipment was acquired in 1995 and it is now impossible to get spare GPS receivers. The PS28 ARCES equipment was acquired in 1999, and it is no longer possible to get spare digitizers. A recapitilization plan for both arrays was submitted to the PTS in October 2008, and installation of new equipment will start in 2010.

U. Baadshaug
S. Mykkeltveit
J. Fyen

References

Kradolfer, U. (1993): Automating the exchange of earthquake information. *EOS, Trans., AGU*, 74, 442.

Kradolfer, U. (1996): AutoDRM — The first five years, *Seism. Res. Lett.*, 67, 4, 30-33.

Mykkeltveit, S. & U. Baadshaug (1996): Norway's NDC: Experience from the first eighteen months of the full-scale phase of GSETT-3. *Semiann. Tech. Summ., 1 October 1995 - 31 March 1996*, NORSAR Sci. Rep. No. 2-95/96, Kjeller, Norway.

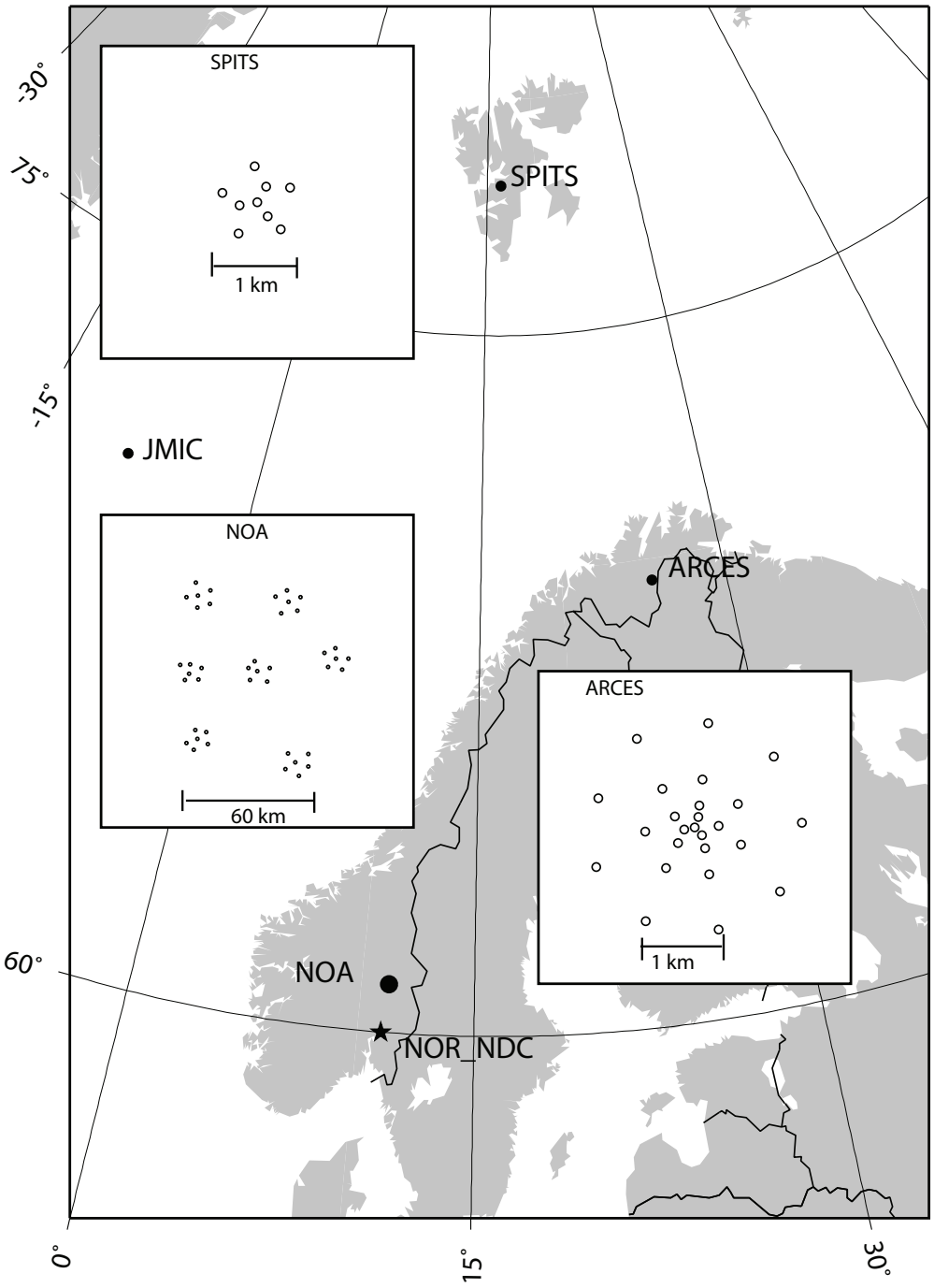

Fig. 4.2.1. The figure shows the locations and configurations of the three Norwegian seismic IMS array stations that provided data to the IDC during the period January - June 2010 The data from these stations and the JMIC three-component station are transmitted continuously and in real time to the Norwegian NDC (NOR_NDC). The stations NOA and ARCES are primary IMS stations, whereas SPITS and JMIC are auxiliary IMS stations.

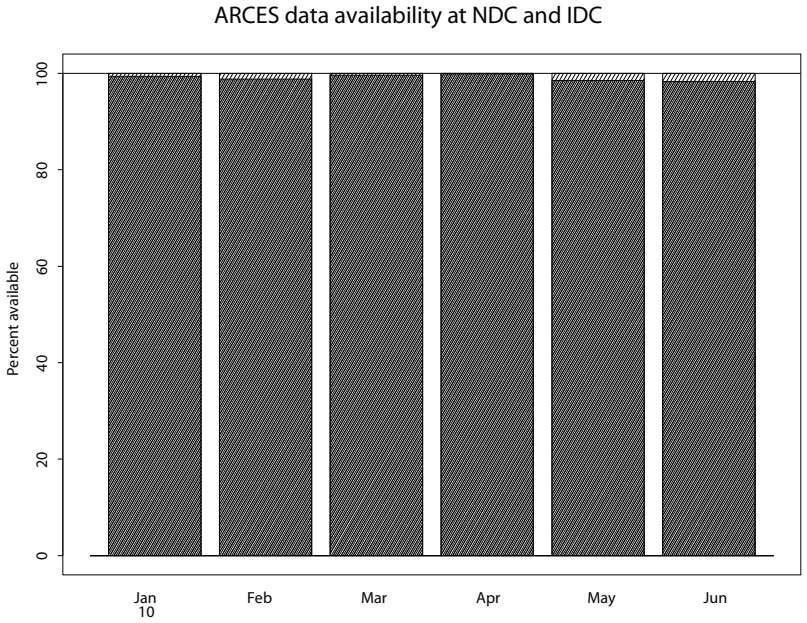

Fig. 4.2.2. The figure shows the monthly availability of ARCES array data for the period January - June 2010 at NOR_NDC and the IDC. See the text for explanation of differences in definition of the term "data availability" between the two centers. The higher values (hatched bars) represent the NOR_NDC data availability.

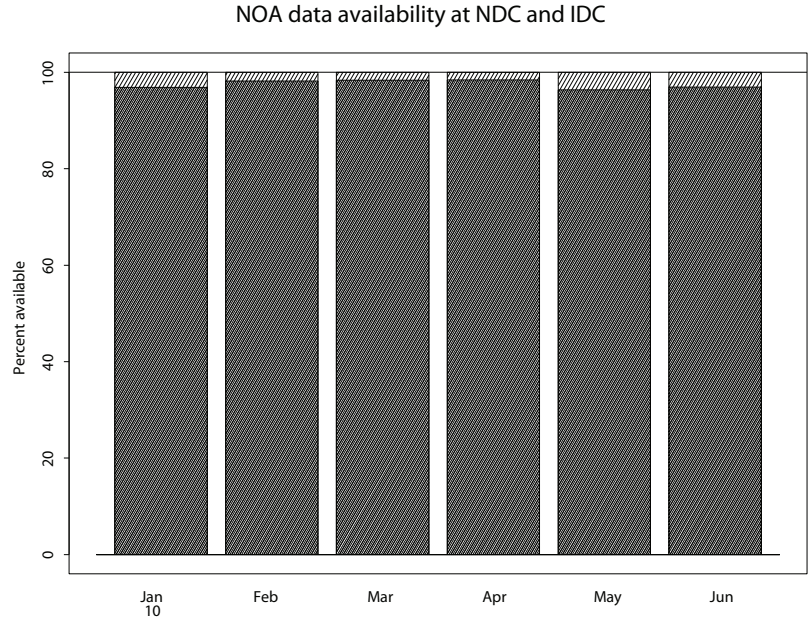

Fig. 4.2.3. The figure shows the monthly availability of NORSAR array data for the period January - June 2010 at NOR_NDC and the IDC. See the text for explanation of differences in definition of the term "data availability" between the two centers. The higher values (hatched bars) represent the NOR_NDC data availability.

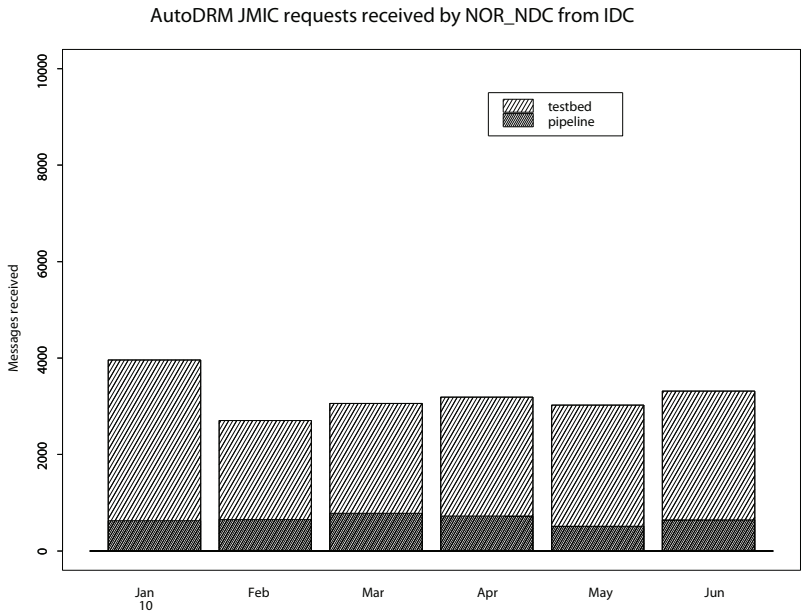

Fig. 4.2.4. The figure shows the monthly number of requests received by NOR_NDC from the IDC for JMIC waveform segments during January - June 2010.

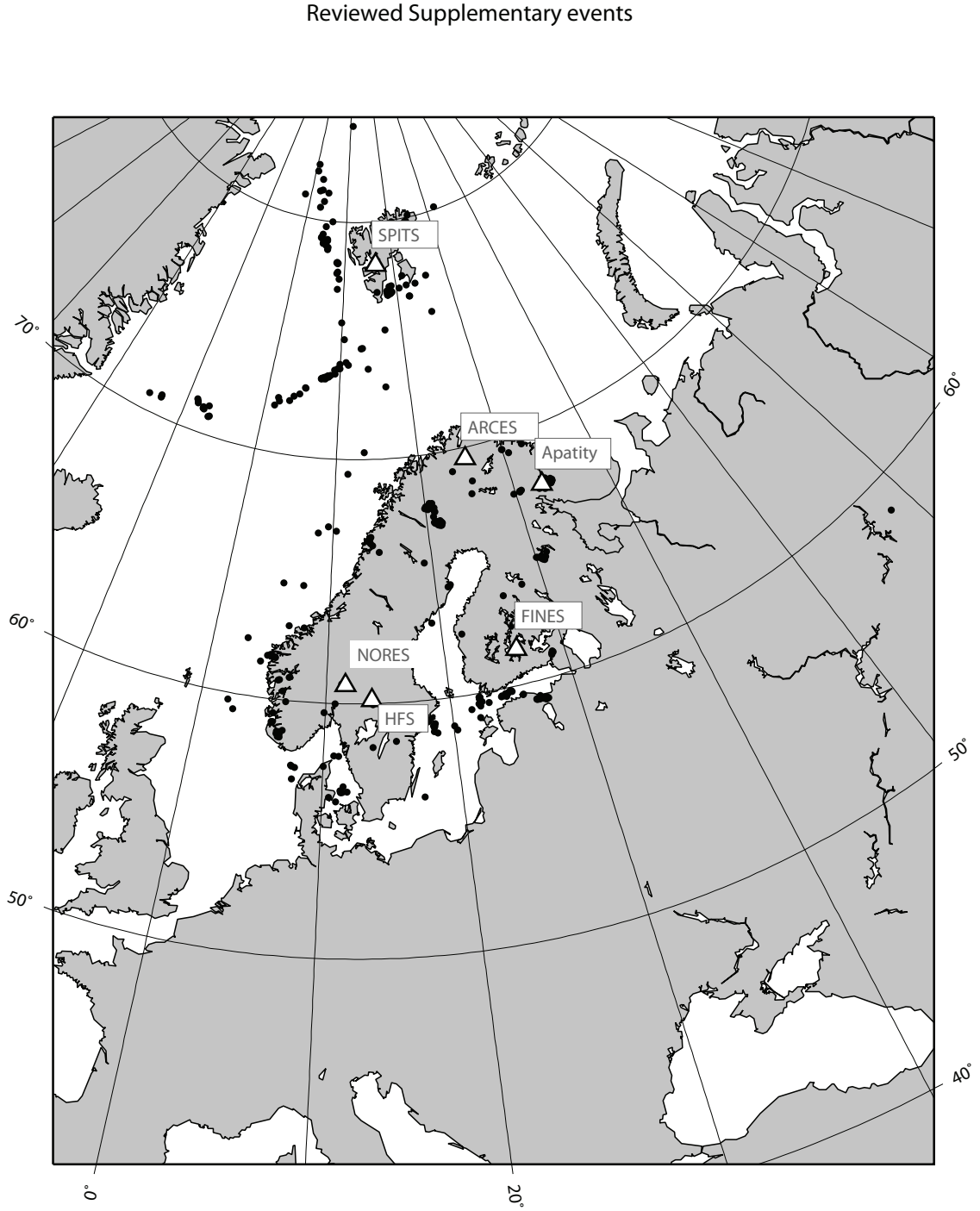

Fig. 4.2.5. The map shows the 458 events in and around Norway contributed by NOR_NDC during January - June 2010 as supplementary (Gamma) events to the IDC, as part of the Nordic supplementary data compiled by the Finnish NDC. The map also shows the main seismic stations used in the data analysis to define these events.

4.3 Field Activities

The activities at the NORSAR Maintenance Center (NMC) at Hamar currently include work related to operation and maintenance of the following IMS seismic stations: the NOA teleseismic array (PS27), the ARCES array (PS28) and the Spitsbergen array (AS72). Some work has also been carried out in connection with the seismic station on Jan Mayen (AS73), the radionuclide station at Spitsbergen (RN49), and preparations for the infrasound station at IS37. NORSAR also acts as a consultant for the operation and maintenance of the Hagfors array in Sweden (AS101).

NORSAR carries out the field activities relating to IMS stations in a manner generally consistent with the requirements specified in the appropriate IMS Operational Manuals, which are currently being developed by Working Group B of the Preparatory Commission. For seismic stations these specifications are contained in the Operational Manual for Seismological Monitoring and the International Exchange of Seismological Data (CTBT/WGB/TL-11/2), currently available in a draft version.

All regular maintenance on the NORSAR field systems is conducted on a one-shift-per-day, five-day-per-week basis. The maintenance tasks include:

- Operating and maintaining the seismic sensors and the associated digitizers, authentication devices and other electronics components.
- Maintaining the power supply to the field sites as well as backup power supplies.
- Operating and maintaining the VSATs, the data acquisition systems and the intra-array data transmission systems.
- Assisting the NDC in evaluating the data quality and making the necessary changes in gain settings, frequency response and other operating characteristics as required.
- Carrying out preventive, routine and emergency maintenance to ensure that all field systems operate properly.
- Maintaining a computerized record of the utilization, status, and maintenance history of all site equipment.
- Providing appropriate security measures to protect against incidents such as intrusion, theft and vandalism at the field installations.

Details of the daily maintenance activities are kept locally. As part of its contract with CTBTO/PTS NORSAR submits, when applicable, problem reports, outage notification reports and equipment status reports. The contents of these reports and the circumstances under which they will be submitted are specified in the draft Operational Manual.

P.W. Larsen
K.A. Løken

5 Documentation Developed

Bungum, H., O. Olesen, C. Pascal, S. Gibbons, C. Lindholm & O. Vestøl (2010): To what extent is the present seismicity of Norway driven by post-glacial rebound? J. Geol. Soc., Vol 167, No. 2, 373-384.

Gharti, H.N., V. Oye, M. Roth & D. Kühn (2010): Automated microearthquake location using envelope stacking and robust global optimization. Geophysics (accepted).

Gibbons, S. & F. Ringdal (2010): Detection and analysis of near-surface explosions on the Kola peninsula. Pure and Appl. Geophys., Vol. 167, No. 4., 413-436.

Gibbons, S., T. Kværna & F. Ringdal (2010): Considerations in phase estimation and event location using small-aperture regional seismic arrays. Pure and Appl. Geophys., Vol 167, No. 4, 381-399.

Hauser, J., K.M. Dyer, M.E. Pasyanos, H. Bungum, J.I. Faleide, S.A. Clark & J. Schweitzer (2010): A probabilistic seismic model for the European Arctic. In: Semiannual Technical Summary, 1 January - 30 June 2010, NORSAR Sci. Rep. 2-2010, Kjeller.

Händel, A., J. Schweitzer & F. Krüger (2010): Local seismicity on and near Bear Island (Norwegian Arctic) from a temporary small aperture array installation in 2008. In: Semiannual Technical Summary, 1 January - 30 June 2010, NORSAR Sci. Rep. 2-2010, Kjeller.

Pirli, M. (2010): NORSAR System Reponse Manual, 2nd Ed., NORSAR, Kjeller, Norway, 180 pp.

Pirli, M., J. Schweitzer, L. Ottemoller, M. Raeesi, R. Mjelde, K. Atakan, A. Guterch, S. Gibbons, B. Paulsen, W. Debski, P. Wiejacz & T. Kværna (2010): Preliminary analysis of the 21 February 2008 Svalbard (Norway) seismic sequence. Seism. Res. Lett., Vol. 81, No. 1, 63-75.

Ringdal, F., T. Kværna, S. Gibbons, S. Mykkeltveit & J. Schweitzer (2010). Basic research on seismic and infrasonic monitoring of the European Arctic. In: Semiannual Technical Summary, 1 January - 30 June 2010, NORSAR Sci. Rep. 2-2010, Kjeller.

Weidle, C., V. Maupin, J. Ritter, T. Kværna, J. Schweitzer, N. Balling, H. Thybo, J.I. Faleide & F. Wenzel (2010): MAGNUS -- a seismological broadband experiment to resolve crustal and upper mantle structure beneath the Southern Scandes mountains in Norway. Seism. Res. Lett., Vol. 81, No. 1, 76-84 (doi: 10.1785/gssrl.81.1.76)

Wilde-Piórko, M., M. Grad, P. Wiejacz & J. Schweitzer (2010): HSPB seismic broadband station in Southern Spitsbergen: First results on crustal and mantle structure from receiver functions and SKS splitting. Polish Polar Research, Vol. 40, No. 4, 301-316 (doi: 10.4202/ppres.2009.16)

6 Summary of technical reports / papers published

6.1 Basic research on seismic and infrasonic monitoring of the European Arctic

Sponsored by Army Space and Missile Defense Command, Contract No. W9113M-05-C-0224

ABSTRACT

This project is a research effort aimed at improving seismic and infrasonic monitoring tools at regional distances, with emphasis on the European Arctic region, which includes the former Novaya Zemlya test site. The project has three main components: a) to improve seismic processing in this region using the regional seismic arrays installed in northern Europe, b) to investigate the potential of using combined seismic/infrasonic processing to characterize events in this region and c) to carry out experimental operation, evaluation and tuning of the seismic threshold monitoring technique.

On 11 November 2009, signals from a magnitude 3.2 event in the eastern Barents Sea were recorded by seismic stations in the Nordic countries and in NW Russia. This part of the Barents Sea has no known history of significant earthquake activity. However, over the past decades, several seismic events at various locations in this region have been detected, and several of these have been confidently associated with anthropogenic activity, like the Kursk submarine accident. As to the source type of the 11 November 2009 event, we are not in a position to draw a firm conclusion. Observations at the ARCES array, at a distance of 800 km, show signal energy up to 40 Hz and show no indication of spectral banding or cepstral peaks. This is quite different from the characteristics of underwater explosions in this area, suggesting that the event is more likely to be an earthquake. This study further illustrates the very efficient high-frequency seismic energy propagation characteristics of the Barents Sea area.

Seismic and infrasound signals at ARCES have recently been associated with blasting at the Suurikuusikko gold mine in northern Finland, approximately 10 km to the west of Hukkakero. This mine started operations in the summer of 2006 and, in order to develop a database of explosions, multi-channel waveform correlation detectors were initiated using ARCES seismic signals as templates. Many hundreds of clear detections have been made indicating several events per week. The absence of detections prior to June 2006, and the absence of detections outside of characteristic times of days, indicate a low false alarm rate. A majority of the over 500 events detected since June 2006 have been associated with infrasound detections at ARCES and at stations of the infrasound networks of Sweden, Finland, and Russia, all at regional distances from the source and with a fortuitous coverage of directions from the mine. While the events appear to be less efficient generators of infrasound than the military munitions explosions at Hukkakero, the blasts occur throughout the year and so will sample a far greater spectrum of atmospheric profiles. Examining long time-series of observations from these well-constrained sources will hopefully improve our understanding of the conditions under which infrasound is observed within and on the edge of the so-called "zone of silence".

International news media reported in July 2009 on an unsuccessful launch of the new Russian intercontinental Bulava missile. The missile was launched from a submarine in the White Sea on 15 July 2009, and was reported to self-destruct during the first stage of flight. The effect of another launch failure of the Bulava missile was visually observed in northern Scandinavia on

9 December 2009, in terms of strange light phenomena in the sky. This caused considerable public attention, and it was reported after some time that the phenomena were believed to originate from an engine failure and self-destruction in the third stage of a Bulava missile. Infrasound signals from both of these launches were well recorded at several infrasound arrays in the region. Array analysis followed by tracing of the estimated back-azimuths located both infrasound sources to the White Sea. During recent years, infrasound signals have been observed in the Nordic region from several rocket launches and meteors entering the atmosphere. Establishing a database of such events is important for future studies of infrasound wave propagation.

6.1.1 Objective

The objective of the project is to carry out research to improve the current capabilities for monitoring small seismic events in the European Arctic, which includes the former Russian test site at Novaya Zemlya. The project has three main components: a) to improve seismic processing in this region using the regional seismic arrays installed in northern Europe, b) to investigate the potential of using combined seismic/infrasonic processing to characterize events in this region and c) to carry out experimental operation, evaluation and tuning of the seismic threshold monitoring technique, with application to various regions of monitoring interest.

6.1.2 Research Accomplished

On 11 November 2009, at 04:18 GMT, signals from a seismic event in the eastern Barents Sea were recorded by seismic stations in the Nordic countries as well as in NW Russia. This part of the Barents Sea has no known history of significant earthquake activity. However, over the past decades, NORSAR has recorded several seismic events at various locations in this region as listed in the NORSAR reviewed regional seismic bulletin. Since January 2006, five small seismic events near Novaya Zemlya have been detected (Table6.1.1 and Fig. 6.1.1).

Table 6.1.1. Seismic events near Novaya Zemlya detected during 01/2006-01/2010

Date	Origin time	Latitude (N)	Longitude (E)	Magnitude (mb)
05/03/2006	23:17:35.7	76.80	66.04	2.65
14/03/2006	20:57:02.4	75.07	53.05	2.23
30/03/2006	10:46:02.8	70.79	51.50	2.30
26/06/2007	03:19:05.0	73.45	53.43	2.75
11/11/2009	04:18:21.0	71.58	46.09	3.20

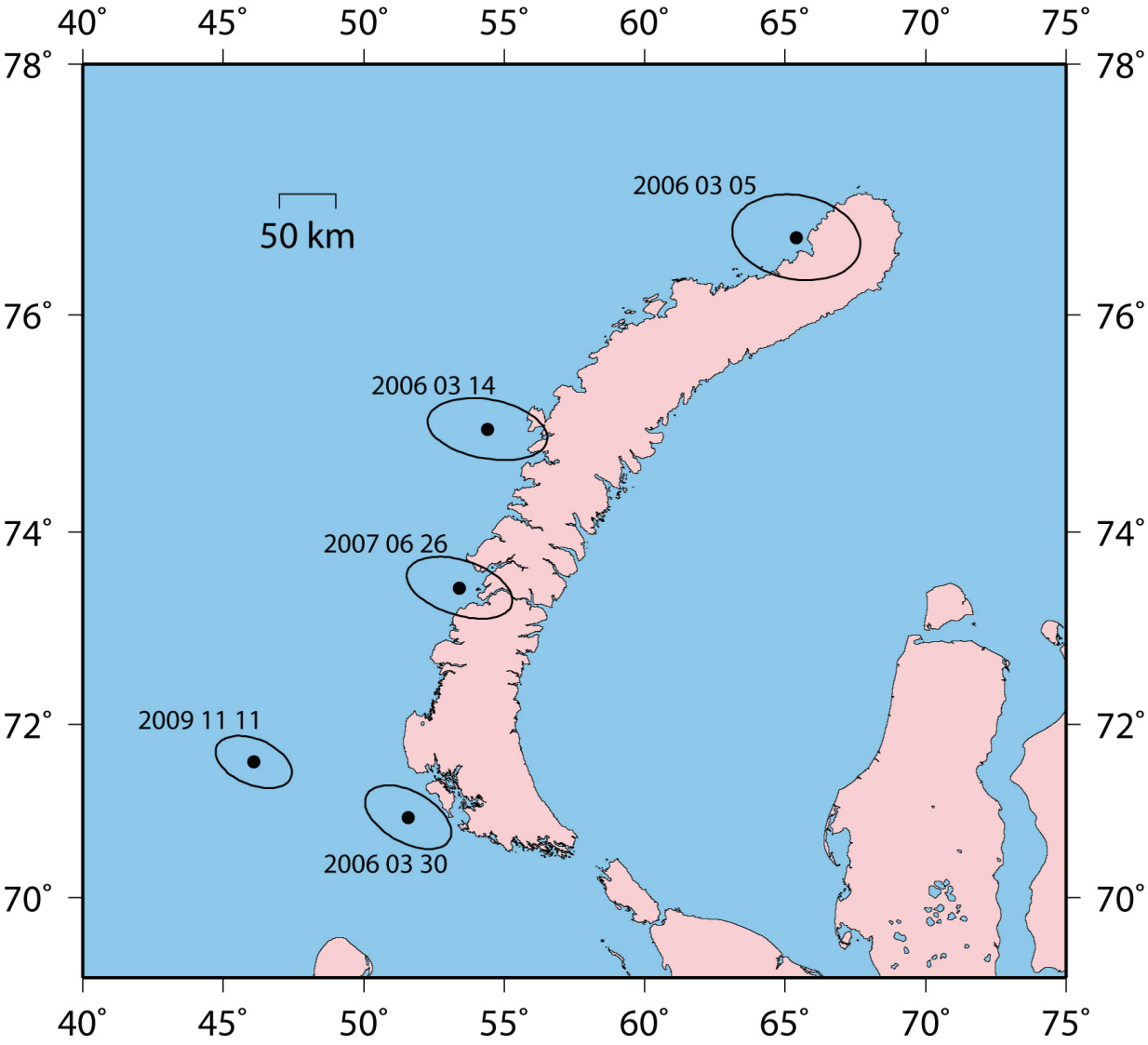

Fig. 6.1.1 Location of seismic events near Novaya Zemlya between 2006 and 2010 as published in the regional NORSAR bulletin. The 95% location confidence ellipses are indicated for each event.

Observations at ARCES

We have analyzed data from the ARCES array in northern Norway recorded for the event on 11 November 2009. Fig. 6.1.2 shows filtered recordings (2-16 Hz) of the three-component center seismometer of ARCES. The characteristics of the traces are similar to previous events from this region, with clear Pn and Sn phases, whereas the Pg and Lg phases are not discernible, at least not in this frequency band. We also note that the direction of the event is nearly due east of ARCES, and that consequently the radial component (se) of the Pn-phase is about as strong as the vertical component, while the Sn phase is by far the most prominent on the transverse (sn) component. This is an important confirmation of the advantages of using the transverse component of the seismogram to increase the probability of detecting S-type phases.

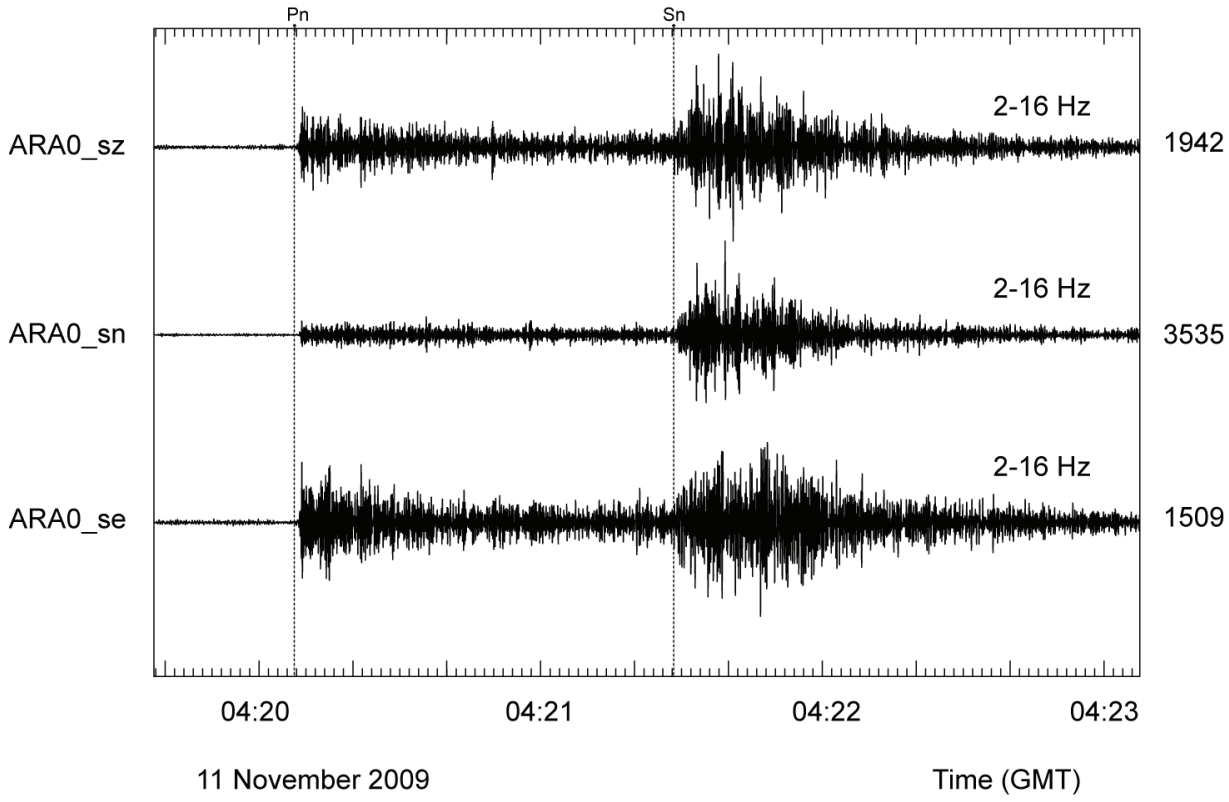

Fig. 6.1.2 Recordings by the three-component center seismometer of the ARCES array of the seismic event in the Barents Sea on 11 November 2009. The traces have been filtered in the 2-16 Hz frequency band.

The event on 11 November 2009 is of special importance since it is the first event near Novaya Zemlya since the high frequency element was installed at ARCES in early 2008. As noted by Ringdal et al. (2008) in their initial study of high frequency ARCES recordings, the available high-frequency data at that time did not include recordings of distant events to the east and north-east of the ARCES array, and the high-frequency propagation from the Novaya Zemlya region to ARCES could therefore not be assessed.

We have therefore made a special analysis of the associated ARCES high frequency recordings for the event on 11 November 2009, as described in Kværna and Ringdal (2010). Fig. 6.1.3 shows shows spectra of the Pn and Sn phases as well as the spectrum of noise preceding the event. We note the significant high-frequency energy of the Pn and Sn phases, with the signal exceeding the noise for frequencies all the way up to 40 Hz for the Pn phase, and even above 40 Hz for the Sn phase.

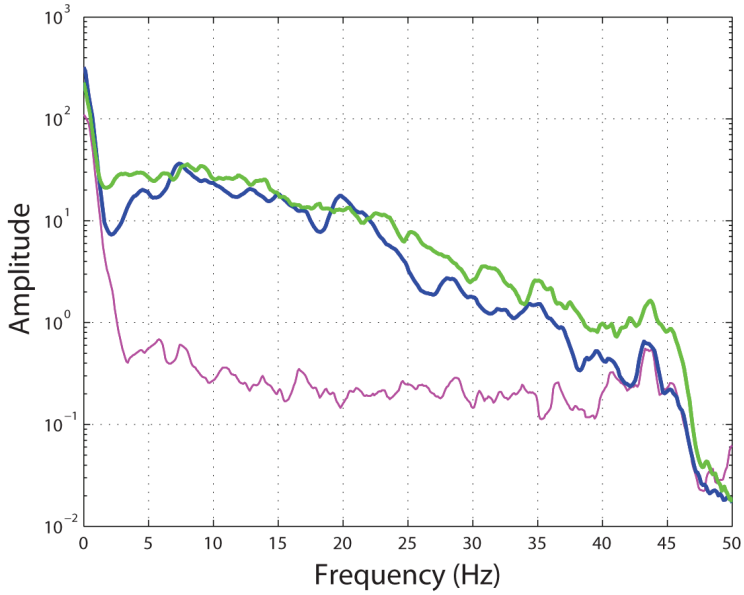

Fig. 6.1.3 Spectra from the ARCES vertical high-frequency element of the Pn (blue) and Sn (green) phases of the 2009 event. The noise spectrum (magenta) preceding the event is also shown.

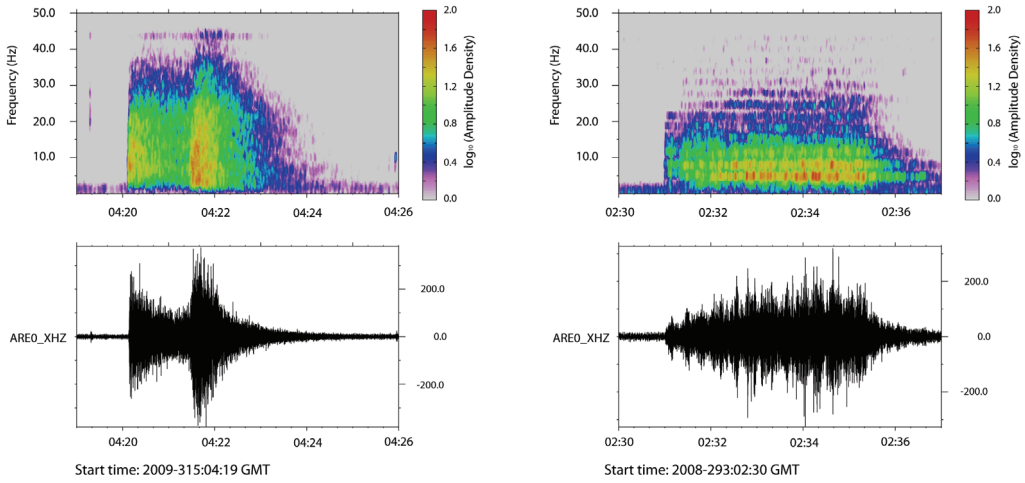

Fig. 6.1.4 Spectrograms from the ARCES vertical high-frequency element of seismic events in the Barents Sea. The left plot shows the seismic event on 11 November 2009. The plot to the right shows a sequence of presumed underwater explosions near the northern coast of the Kola Peninsula on 19 October 2008. The traces have been high-pass filtered at 2.2 Hz. Note the significant differences between the two plots.

After the ARCES high-frequency element was installed, there have been a number of seismic events in or near the mining regions of NW Russia. However, the distance from ARCES to these events are 300 km or less, whereas the epicentral distance of the 11 November 2009 event was as large as 800 km. Nevertheless, it is of interest to compare the latter event to some of the presumed underwater explosions at about 300 km distance. One way to make such a comparison is illustrated in Fig. 6.1.4. This figure shows spectrograms from the ARCES vertical high-frequency element of the 11 November 2009 event as well as a sequence of presumed

underwater explosions near the northern coast of the Kola Peninsula on 19 October 2008. We note that the presumed explosions in 2008 have their dominant energy at much lower frequencies than the event in 2009, even though the latter event is at a much larger distance from ARCES. The spectral scalloping evident in the 2008 plot is typical of many underwater explosions, and is associated with multiple reflections from the bottom and surface of the water (e.g. Baumgardt and Der, 1998).

Kværna and Ringdal (2010) applied the software described by Oberg et al. (2004) to compare the cepstral peaks associated with various categories of events in the Barents Sea region. They concluded that the recordings from the 11 November 2009 event were more consistent with previous earthquake recordings than with recordings of known underwater explosions, although they noted that it is difficult to discriminate reliably using this criterion only.

Infrasound studies

The site of military explosions at Hukkakero, northern Finland (67.934 N, 25.832 E) has raised significant interest in recent years due to the generation of infrasound (Gibbons et al., 2007). Hukkakero is the site of between 20 and 50 near-surface explosions every year for the destruction of expired ammunition. The events occur on consecutive days in August and September and provide a useful data set for the study of infrasound propagation for a number of reasons:

- The location of the events is known. All explosions are known to take place within approximately 300 meters of the coordinates stated.
- The sources are almost identical both in terms of yield (approximately 20000 kg per explosion) and source-time function (there are no multiple or ripple-fired explosions as are common in open-cast mining: see, for example, Gibbons et al., 2007).
- The similarity of the waveforms makes the events amenable to detection using waveform correlation detectors (Gibbons and Ringdal, 2006). This means that every event can be detected with an almost negligible false alarm rate and also that the origin times of explosions can be constrained very accurately.

On October 2, 2009 we noted an event which occurred shortly after the end of the 2009 Hukkakero explosion sequence and was reported by the NORSAR Event Warning System (Schweitzer, 2003). Due to the event origin time and poor signal correlation with known events, this event was deemed unlikely to be from the same source location. Using seismic waveforms from stations of the Finnish national seismic network, in addition to ARCES, indicated an event location approximately 10 km to the west of the Hukkakero site. A consultation with colleagues at the Institute of Seismology at the University of Helsinki concluded that the source of the October 2 event was almost certainly the Kittilä Gold Mine, operated by Agnico-Eagle, at Suurikuusikko (67.90 N, 25.39 E). Fig. 6.1.5 displays the location of the sources together with waveforms from one event from each of the two explosion sites.

The magnitude estimate for the seismic event on October 2, 2009, was just in excess of 1.0 and, while such events are routinely detected and included in the fully automatic seismic event bulletins at NORSAR, they are not large enough to be reviewed manually and included in the pub-

lished analyst bulletin. We therefore use a correlation detector to try to catch as many occurrences as possible of seismic events at this mine.

Gibbons and Ringdal (2006) demonstrated that seismic arrays have a tremendous advantage over single stations for correlation detectors. Firstly, there is a great suppression of the background noise made possible by a stacking of the correlation coefficient traces. Secondly, we can perform a post-processing of detections by examining the alignment of the cross-correlation coefficients from the different channels and large numbers of false alarms can be eliminated in this way.

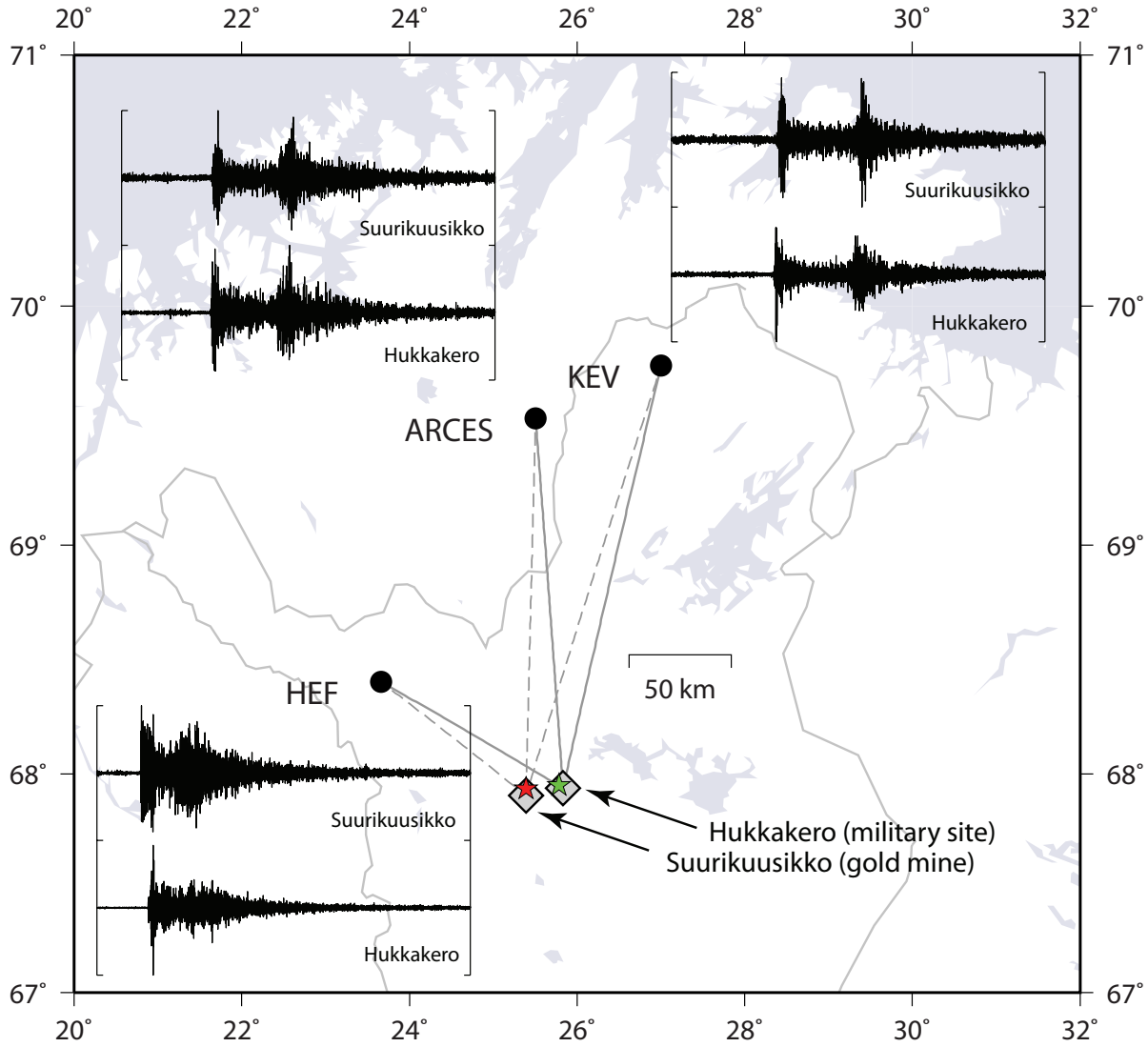

Fig. 6.1.5 Locations of the Hukkakero military explosion site (67.934 N, 25.832 E) and the Suurikuusikko gold mine (67.902 N, 25.391 E) in relation to the ARCES seismic array and the HEF and KEV 3-component stations of the Finnish seismic network. Two minutes of data are displayed for each trace beginning at the estimated event origin time and all waveforms are bandpass filtered 3-16 Hz. The green and red stars denote event location estimates for a Hukkakero and a Suurikuusikko event respectively using the network displayed.

Fig. 6.1.6 displays all of the detections attained since 2006 using a correlation detector with signal at ARCES from the October 2, 2009, event as a template. A total of 493 detections have been made in the period shown. No convincing detections have been made prior to July 2006, and a consultation with the information provided by Agnico-Eagle confirms that this is consistent with operational history of the mine. The detections displayed in Fig. 6.1.6 have yet to be screened manually for false alarms, but have been filtered using the criteria described by Gibbons and Ringdal (2006). The concentration of detections at particular times of day and the absence of detections at night time suggest that the false alarm rate is very low.

The detection of infrasound signals at ARCES following many events in this sequence indicates that this source may be of great interest for the study of sound propagation of regional distances. The mine location is fortuitous in relation to the network of infrasound sensors in Norway, Sweden, Finland and Russia (Fig. 6.1.7) which provide an almost optimal coverage of the different directions from the source. Some of the stations are located either at the edge of or well within the so-called "Zone of Silence" within which the propagation of infrasound is currently very poorly understood. While initial indications are that the Suurikuusikko mine is a less efficient generator of infrasound than the military explosions at Hukkakero, the new data set has a great advantage in that the events occur throughout the year, and so will sample many different atmospheric profiles, and may contribute more to understanding the conditions under which infrasound is observed from explosions at a known location.

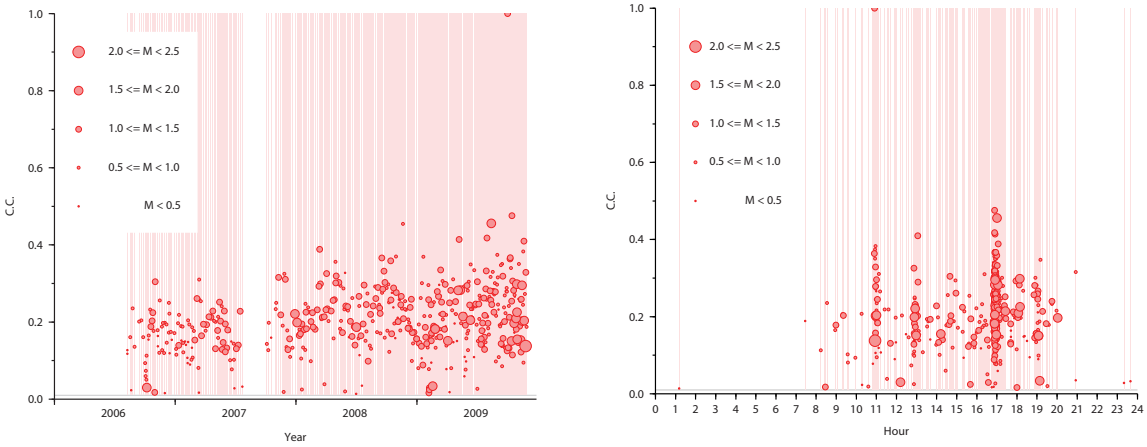

Fig. 6.1.6 Correlation detections on the ARCES array using a template of the signal from the October 2, 2009, event. The left plot shows detections chronologically, the right plot shows detections by local time of day at ARCES. The detector was run on archived data from years prior to 2006 and the very few detections prior to July 2006 were all demonstrated to be false alarms. The time-of-day plot shows very clear clusters of events close to 1100, 1300, 1700 and 1900 hours. There are almost no detections between 2000 and 0800 hours which also suggests that the false alarm rate among these detections is probably very low.

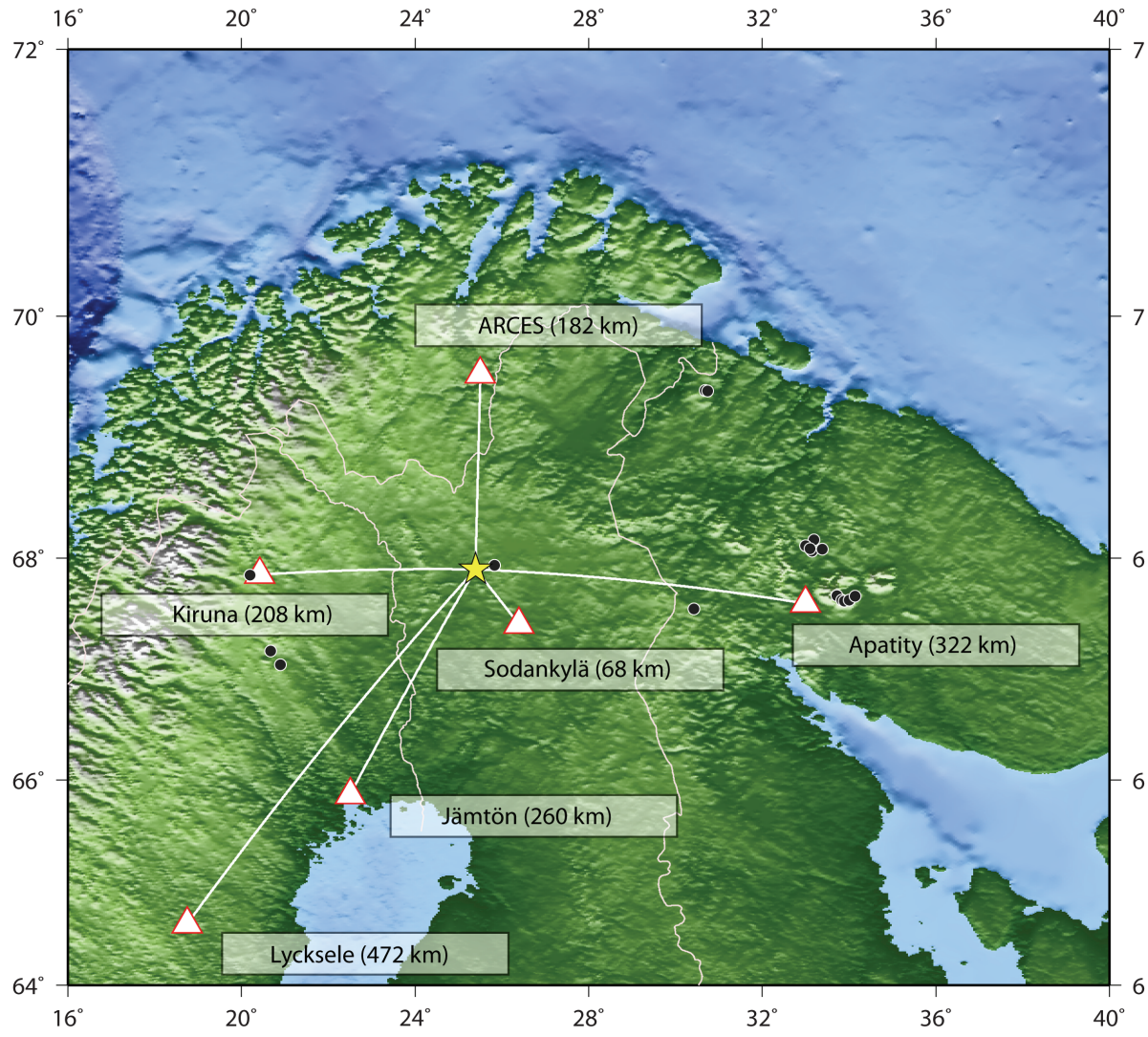

Fig. 6.1.7 Location of the Suurikuusikko gold mine in Central Lapland in relation to the ARCES and Apatity seismic/infrasonic arrays and the microphone arrays at Kiruna, Lycksele, Jämtön and Sodankylä.

The Sodankylä microphone array is located at only 68 km from the source (to the south). This station is located within the so-called "zone of silence" although it is accepted that infrasound can propagate to these distances in the lower atmosphere (the troposphere) given favorable wind and temperature profiles. Very clear infrasound signals have been observed for many of these events at Sodankylä (see Fig. 6.1.8) and it will be the subject of future research to understand the conditions under which infrasound is and is not detected at this and the other stations shown.

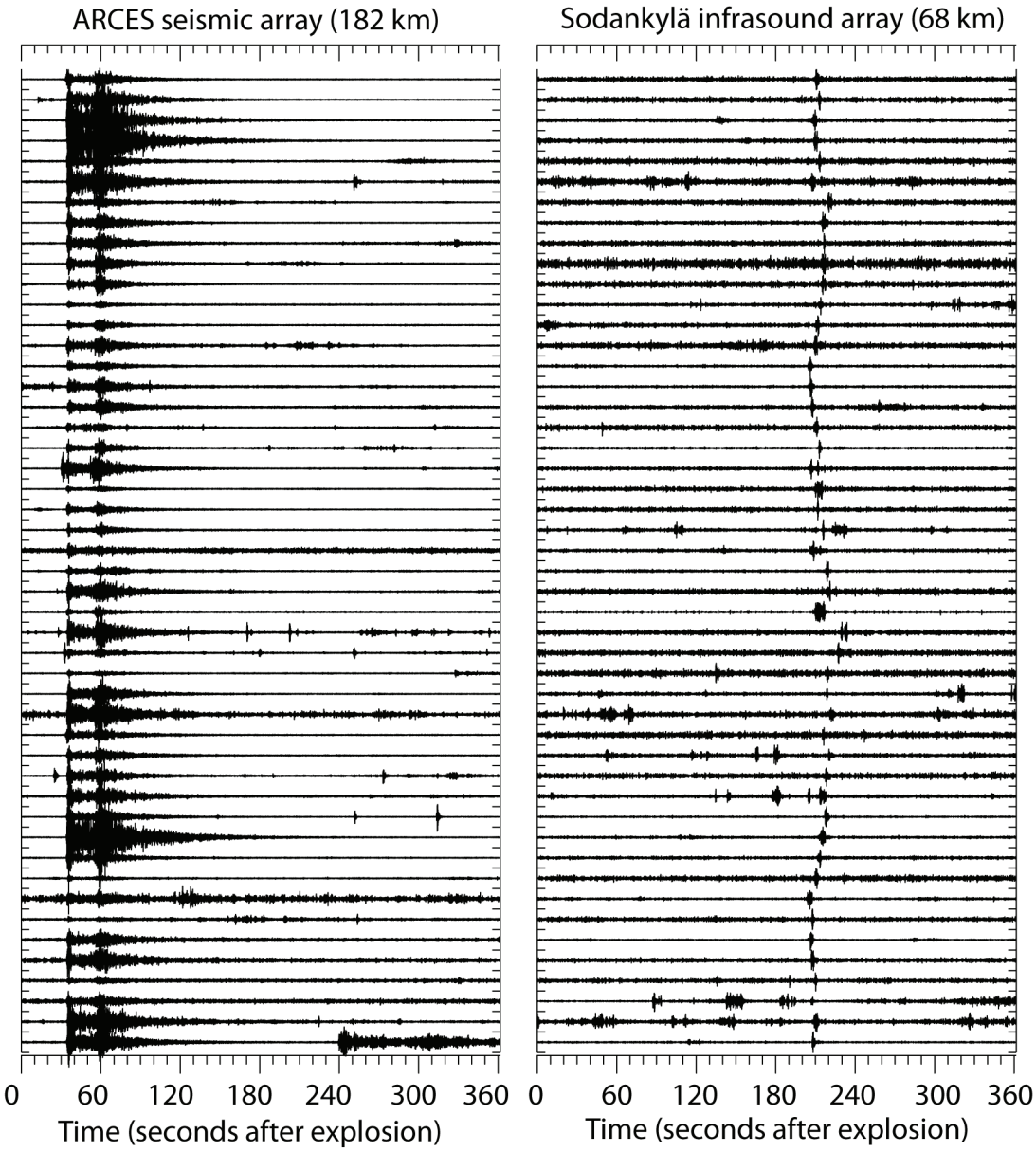

Fig. 6.1.8 Waveforms at the ARCES seismic array (ARA0_sz channel, bandpass filtered 4-16 Hz) and the Sodankylä microphone array (SDA1_MI channel, bandpass filtered 2-5 Hz) for the 50 events with the greatest coherence of the associated infrasound signals. The ARCES waveforms are drawn to a common scale, demonstrating the variation in the event magnitudes. Each channel of the Sodankylä data is scaled individually. (Note that infrasound signals at ARCES arrive later than displayed here.)

Infrasound recordings of the Bulava Missile

International news media reported in July 2009 on an unsuccessful launch of the new Russian intercontinental Bulava missile. The missile was launched from a submarine in the White Sea on 15 July. Infrasound signals associated with this launch were recorded at NORSAR's experimental infrasound station at ARCES (Roth et al., 2008) and the four stations in Sweden and Finland operated by the Swedish Institute of Space Physics (IRF). Another Bulava launch took place on 9 December 2009. Around 6:50 UTC on that day, strange light phenomena were

observed in northern Norway. These observations caused a lot of attention in the news media, and after a while it became evident that the phenomena were associated with this launch. According to the Russian Defence Ministry there was an engine failure in the third stage of the flight that caused the problem. According to recent information provided by the Norwegian Ministry of Defence, they believe that the missile exploded at an altitude between 100 and 300 km above the Novaya Zemlya region, and that the missile was launched from a submarine in the north-eastern part of the White Sea. Infrasound signals believed to originate from this missile launch were observed at ARCES as well as at the infrasound station in Apatity on the Kola peninsula. No infrasound signals were found at the stations of the IRF network for the 9 December event.

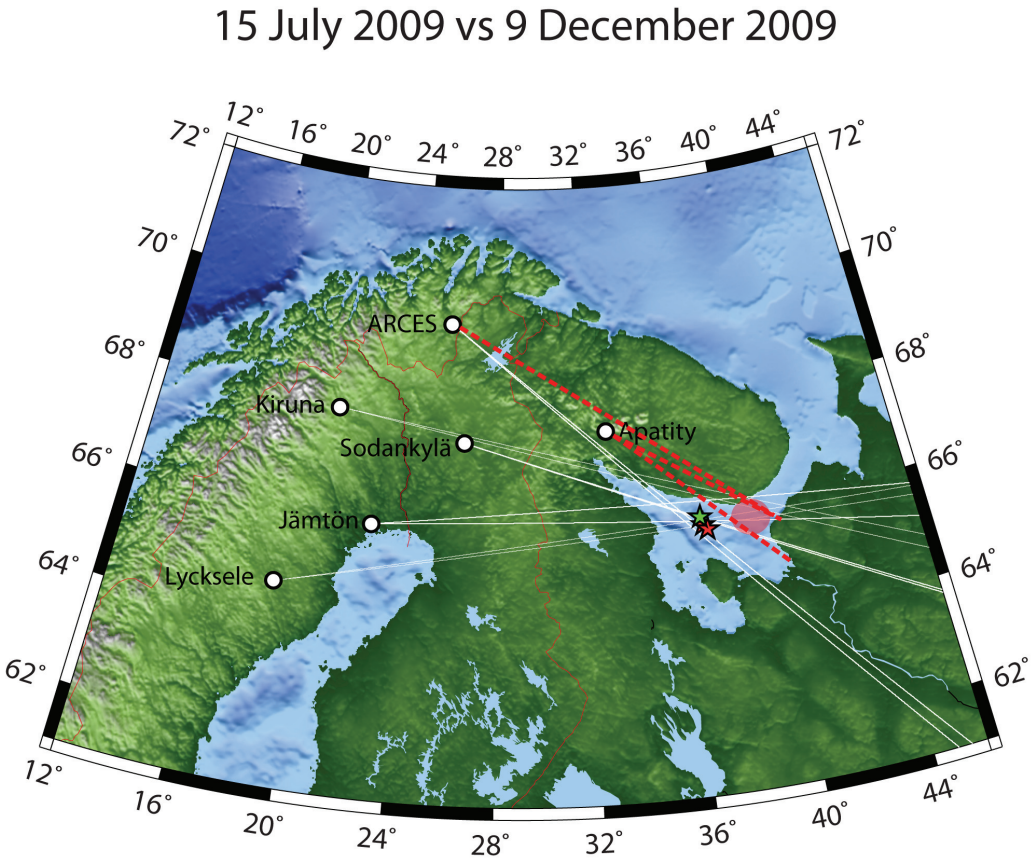

Fig. 6.1.9 The dashed red lines show estimated back-azimuths from the ARCES and Apatity infrasound arrays for the 9 December 2009 event. See text for details.

Fig. 6.1.9 shows the results of our analysis of these two events. The approximate source region of the 9 December event is indicated by the red ellipse. For comparison, the red and green stars show the estimated locations of the 15 July 2009 event. The red stars show locations provided by Prof. L. Liszka of the Swedish Institute of Space Physics, and the green star is from the study by Kværna (2010).

6.1.3 Conclusions and Recommendations

Seismic events in the eastern Barents Sea are rare, and the event on 11 November 2009 is therefore of considerable interest. It is the first recorded seismic event in this region since the new high-frequency system was installed at the ARCES array on 23 March 2008. Our analysis of this event confirms the preliminary results of Ringdal et al. (2008) that there is a remarkably efficient propagation from regional events recorded at ARCES at frequencies up to 30 Hz and above.

This result is similar to what has been previously observed at the Spitsbergen array for paths from Novaya Zemlya crossing the Barents Sea. The Spitsbergen studies showed that energy up to 30 Hz and above can be recorded with good signal-to-noise ratio even for small events at epicentral distances as large as 1000 km and we see a similar result in this study, although the event is at a slightly shorter distance (800 km). We consider that there is still much to be gained by making improved use of the high-frequency recordings in the European Arctic, and we recommend that a systematic mapping of the high-frequency propagation characteristics of this region be undertaken.

As discussed by Ringdal et al. (2008), there are several advantages of high-frequency recordings in a nuclear monitoring context. Although the best filter band for event detection over paths across the Barents region generally appears to be either 4-8 Hz or 8-16 Hz, the most remarkable result shown in our previous papers as well as the current study is the strong SNR even at the highest frequencies (up to 40 Hz). While such frequencies would not be used for detection purposes, the high frequency data could be very important for signal characterization, as also pointed out by Bowers et. al. (2001) in their paper discussing the level of deterrence to possible CTBT violations in the Novaya Zemlya region provided by data from the Spitsbergen array. In fact, it appears from the present study that similar advantages are provided by the ARCES array.

The infrasound databases that have been developed based on the explosions in northern Finland provides a unique resource for studies of infrasonic propagation under controlled conditions. One of the main topics to be studied is the surprising observations of various infrasound phases in what is often denoted a “zone of silence” (less than 200 km distance). We plan to carry out various modelling exercises in order to further investigate the propagation of infrasound phases at local distances. At the same time we recommend that the ongoing accumulation of ground truth data of a variety of infrasound sources should be continued.

During recent years, infrasound signals been observed in the Nordic region from several rocket launches and meteors entering the atmosphere. Establishing a database of such events is important for future studies of infrasound wave propagation.

References

Baumgardt, D.R. and Der, Z. (1998). Identification of presumed shallow under-water chemical explosions using land-based regional arrays. Bull. Seism. Soc. Am. 88, pp. 581-595.

Bowers, D., P. D. Marshall, and A. Douglas (2001). The level of deterrence provided by data from the SPITS seismometer array to possible violations of the Comprehensive Test Ban in the Novaya Zemlya region, *Geophys. J. Int.*, 146, pp. 425-438.

Gibbons, S. J. and Ringdal, F. (2006). The detection of low magnitude seismic events using array-based waveform correlation, *Geophysical Journal International*, **165**, 149-166.

Gibbons, S. J., Ringdal, F. and Kværna, T. (2007). Joint seismic-infrasonic processing of recordings from a repeating source of atmospheric explosions. *Journal of the Acoustical Society of America*, **122**, EL158-EL164.

Kværna, T. (2010). Infrasound signals from recent rocket launches in the White Sea. *In NORSAR Scientific Report No. 1-2010: Semiannual Technical Summary, NORSAR, Kjeller, Norway.* pp. 35-43.

Kværna, T., and Ringdal, F. (2010). Seismic event in the eastern Barents Sea, 11 November 2009. *In NORSAR Scientific Report No. 1-2010: Semiannual Technical Summary, NORSAR, Kjeller, Norway.* pp. 26-34.

Oberg, D., Kværna, T. and Ringdal, F. (2004). Discriminants for seismic monitoring. *In NORSAR Scientific Report No. 2-2004: Semiannual Technical Summary, NORSAR, Kjeller, Norway.* pp. 57-69.

Ringdal, F., Kværna, T., and Gibbons, S. J. (2008). Initial studies of high-frequency signals recorded at ARCES. *In NORSAR Scientific Report No. 2-2008: Semiannual Technical Summary, NORSAR, Kjeller, Norway.* pp. 27-51.

Roth, M., Fyen, J., and Larsen, P. W. (2008). Setup of an experimental infrasound deployment within the ARCES array. *In NORSAR Scientific Report No. 2-2008: Semiannual Technical Summary, NORSAR, Kjeller, Norway.* pp. 52-59.

Schweitzer, J. (2003). NORSAR's Event Warning System (NEWS), *In NORSAR Scientific Report No. 1-2003: Semiannual Technical Summary, NORSAR, Kjeller, Norway.* pp. 27-32.

Frode Ringdal
Tormod Kværna
Steven J. Gibbons
Svein Mykkeltveit
Johannes Schweitzer

6.2 Seismic Monitoring of the North Korea Nuclear Test Site Using Multi-Channel Waveform Correlation on the Matsushiro Array (MJAR) in Japan

6.2.1 Introduction

The Democratic People's Republic of Korea (DPRK) announced on 25 May 2009 that it had conducted its second nuclear test, the first one having taken place on 9 October 2006. As was the case with the first test, the second test was detected automatically, located and reported by the International Data Center (IDC) of the Comprehensive nuclear Test-Ban-Treaty Organization (CTBTO). The only primary seismic array within 1000 km of the test site which was in IDC operations at the times of both nuclear tests[1] is the Matsushiro array, MJAR, in Japan, at a distance of approximately 950 km. The location of MJAR with respect to the test site and the other IMS seismic stations in the region is displayed in Figure 6.2.1. Despite high SNR signals from both 2006 and 2009 events, MJAR failed on both occasions to report a detection with a qualitatively correct phase classification and backazimuth estimate. Because of this, although arrival time measurements at MJAR could be used to constrain the reviewed event location estimates, the array did not contribute to the fully automatic preliminary event locations. Signals at MJAR are notoriously incoherent, even at relatively low frequencies for signals from events at teleseismic distances (Kato et al., 2005). The incoherency problems are likely to be exacerbated for the more dispersed, high-frequency regional arrivals. Gibbons et al. (2008) demonstrated that, due to the relatively large array aperture, an incoherent slowness estimate for regional Pn phases may me more effective than attempting coherent f-k analysis.

The similarity between the signals from the two nuclear tests has been noted in numerous studies. In particular, the ripple-for-ripple likeness at many stations has allowed very accurate relative time measurements to be made for high-precision relative event location estimates. Wen and Long (2010), using differential time measurements from stations at regional distances, obtained a location for the 2009 test which was ~2.2 km to the west and ~0.7 km to the north of the 2006 test. Selby (2010), using an entirely distinct network of stations - a set of primary IMS seismic arrays at teleseismic distances, concluded a relative location of ~1.8 km to the west and ~0.3 km to the north, but points out that the two relative locations are consistent to within the appropriate uncertainties. While MJAR was not one of the IMS seismic arrays selected by Selby (2010), the upper panel of Figure 6.2.2 demonstrates great similarity between the two signals. In particular, we note that the similarity between the signals from the two events on a single sensor is far greater than the similarity between two signals from the same event on different sensors. This is almost surprising considering that the three channels displayed, MJA0_HHZ, MJA1_HHZ, and MJA2_HHZ, are separated by distances of 1.1 km, 1.65 km, and 1.60 km; of the same order as or less than the estimated distance between the two event epicenters.

1. The KSRS array in South Korea also recorded the first test, but was not certified until November 2006 and data from this station were not available in the operational pipeline at the IDC on October 9, 2006.

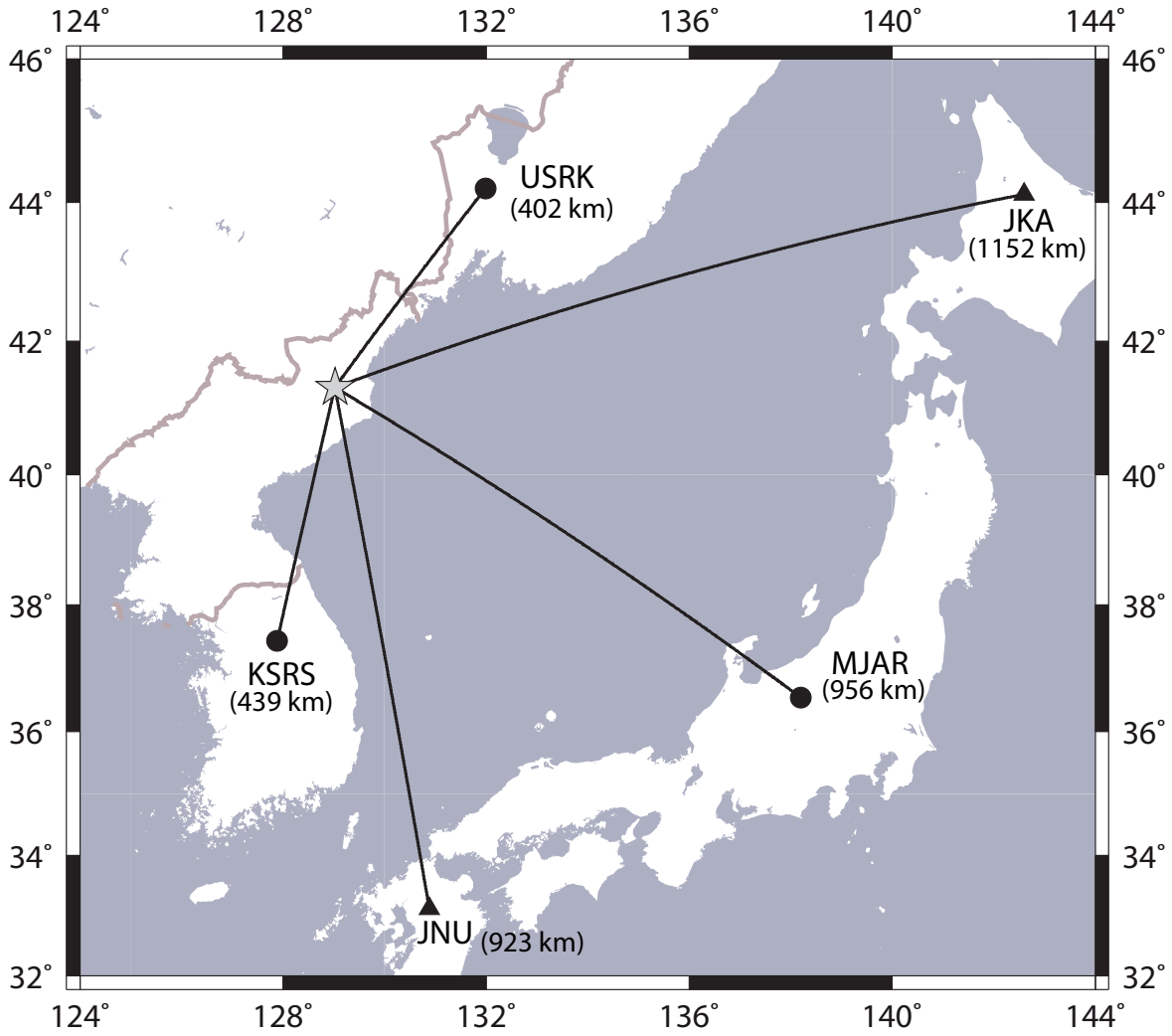

Fig. 6.2.1. Location estimate for the May 25, 2009, North Korea nuclear test with respect to the closest five IMS stations. Circles indicate primary seismic array stations and triangles indicate auxiliary 3-component stations.

The lower panel of Figure 6.2.2 indicates that the values of the correlation coefficient (or rather a related detection statistic which will be defined precisely in the next section) at the time of the optimal match are significantly greater than the background values, making the monitoring situation a candidate for a full waveform correlation detection study. This is to say that we take a signal template for the 2006 test, and correlate this with continuous MJAR data according to the formulation of Gibbons and Ringdal (2006). We need to assess a) the potential for automatically detecting subsequent nuclear tests at that site and b) monitoring the false alarm rate associated with such a detection scheme.

Spectral analysis on the MJAR signals indicate that the best frequency band is likely to be 2 - 8 Hz. In the correlation procedure described here, all waveforms are bandpass filtered in this frequency band prior to the correlation.

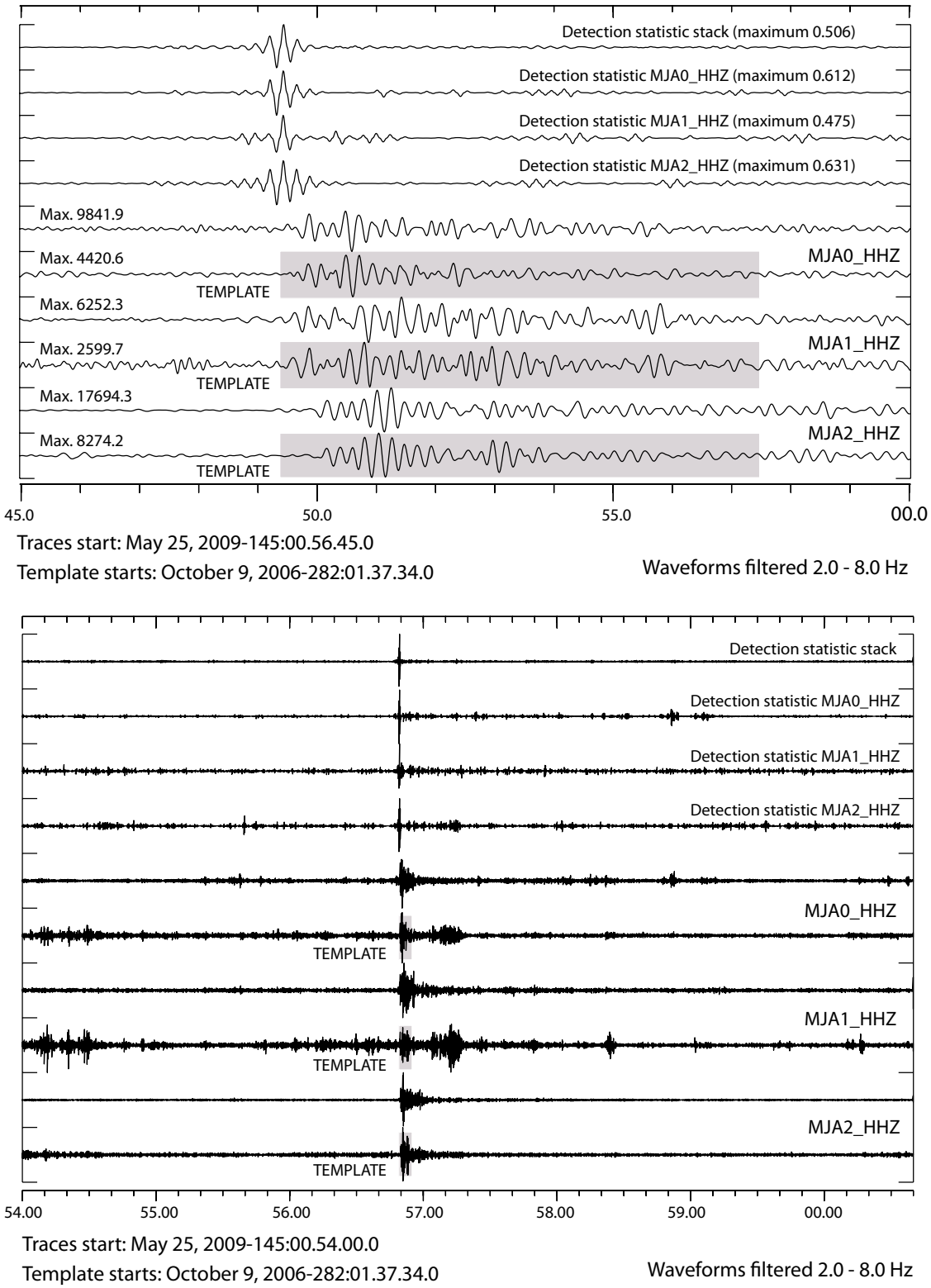

Fig. 6.2.2. Waveforms from three channels of the MJAR array from the May 25, 2009, DPRK nuclear test aligned with the corresponding waveforms from the October 9, 2006, event. The corresponding individual channel detection statistic traces are displayed together with the array stack. The upper panel is a close-up of the lower panel.

6.2.2 A Multi-Channel Correlation Detection Procedure

Formulation

The vector of ***N*** consecutive time-samples containing the waveform template recorded on sensor ***i*** is denoted x_i , where it is understood that the data is scaled a priori to give a unit norm:

$$|\boldsymbol{x}_i| = 1. \qquad (6.2.1)$$

If $y_i(t)$ denotes the vector of ***N*** consecutive time-samples starting at time ***t*** on sensor ***i*** then

$$C_i(t) = \frac{(\ \boldsymbol{x}_i.\boldsymbol{y}_i(t)\ )\,\mathrm{abs}(\ \boldsymbol{x}_i.\boldsymbol{y}_i(t)\ )}{(\ \boldsymbol{y}_i(t).\boldsymbol{y}_i(t)\ )} \qquad (6.2.2)$$

provides a signal-specific detection statistic for this single sensor indicating the degree of similarity between the unit-norm template vector and the time-series beginning at time ***t***. $C(t)$ resembles the square of the fully-normalized correlation coefficient (avoiding the computational expense of calculating the square roots for each sample) but maintains the sign such that the array detection statistic for ***M*** sensors

$$C(t) = M^{-1}\sum_{i=1}^{M} C_i(t) \qquad (6.2.3)$$

results in cancellation in the absence of alignment of features in the individual traces.

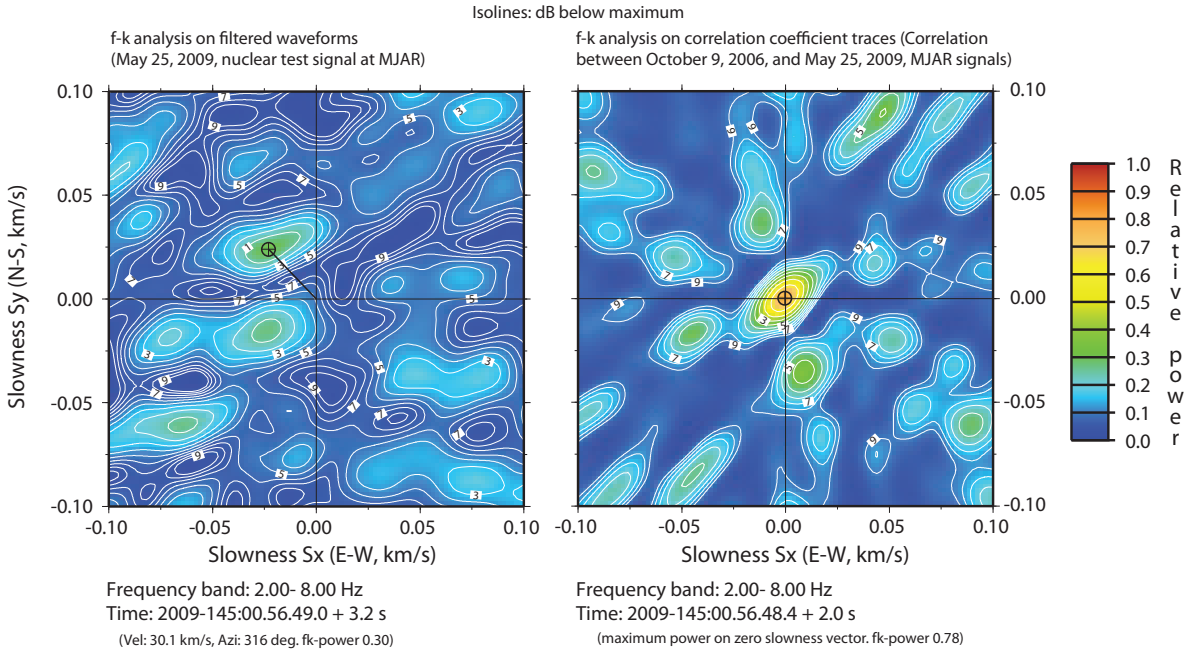

Fig. 6.2.3. Frequency-wavenumber spectrum on the MJAR array of (left) a 3.2 second long data window for Pn arrival for the May 25, 2009, test and (right) for the single channel detection statistic traces for a 2.0 second window centered at the time of the local maximum (see Fig. 6.2.2). Note that the relative power in the right hand panel is far higher than that in the left indicating that the incoming wavefront corresponds far better with the waveform template than with a plane wavefront model. The zero slowness vector in the right hand panel indicates that the incoming and template wavefronts approached the array from the same direction (Gibbons and Ringdal, 2006). Note that the slowness estimate inferred in the left panel is not consistent qualitatively with the predicted arrival from the North Korea test site.

Most importantly, given a detection on C(t), performing frequency-wavenumber or f-k analysis (e.g. Capon, 1969; Kennett, 2002) on the individual detection statistic traces, $C_i(t)$, allows any detection resulting from coincidental similarity between two wavefronts approaching from slightly different directions to be screened out automatically (Gibbons and Ringdal, 2006; see Figure 6.2.3, right hand panel). This post-processing step would not be possible had the sign information been lost, and has been demonstrated to filter out the vast majority of false alarms when detecting events from a source of repeating seismicity even when there is significant waveform dissimilarity between subsequent events (e.g. Gibbons and Ringdal, 2010).

Any detector requires a threshold which must be exceeded in order for a detection to be reported. In this study we follow an idea similar to that of Shelly et al. (2007) where triggers are identified as outliers to the distribution of the detection statistic in a given time-interval. Firstly, the statistic C(t) is evaluated over a window of continuous data, typically of length close to 20 minutes. Secondly, the extreme 1% of these values are removed and the standard deviation of the remaining values calculated. Finally, the ratio between C(t) and this standard deviation is returned and referred to here as the ‘‘***Detection statistic SNR***’’.

Results for the period January 1, 2006, to June 20, 2009.

All values of the detection statistic SNR exceeding 5.0, for which the f-k analysis also resulted in an almost-zero slowness vector, were reported. Based upon the frequency-wavenumber spectrum displayed in the right hand panel of Fig. 6.2.3, a detection was passed if the implied slowness did not exceed 0.01 s/km and if the relative power exceeded 0.20. These detections are displayed in Figure 6.2.4 as a function of time.

Table 6.2.1. Number of detections obtained between January 1, 2006, and June 20, 2009, as a function of the required detection statistic ratio.

Ratio threshold	Number of detections
14.0	2
13.0	3
12.0	3
11.0	4
10.0	7
9.0	20
8.0	88
7.0	356
6.0	1248
5.0	3632

The number of detections reported for different thresholds of this ratio are displayed in Table 6.2.1 and it is clear both here and in Figure 6.2.4 that the May 25, 2009, event was detected using correlation on MJAR data with a far higher greater value of the detection statistic than at

any other time during this period of over 3 years. With an appropriate and conservative detection threshold, the 2009 test could have been detected from the template of the 2006 test with no false alarms. However, for any kind of robust monitoring of a given source region, we need to allow for considerable waveform dissimilarity.

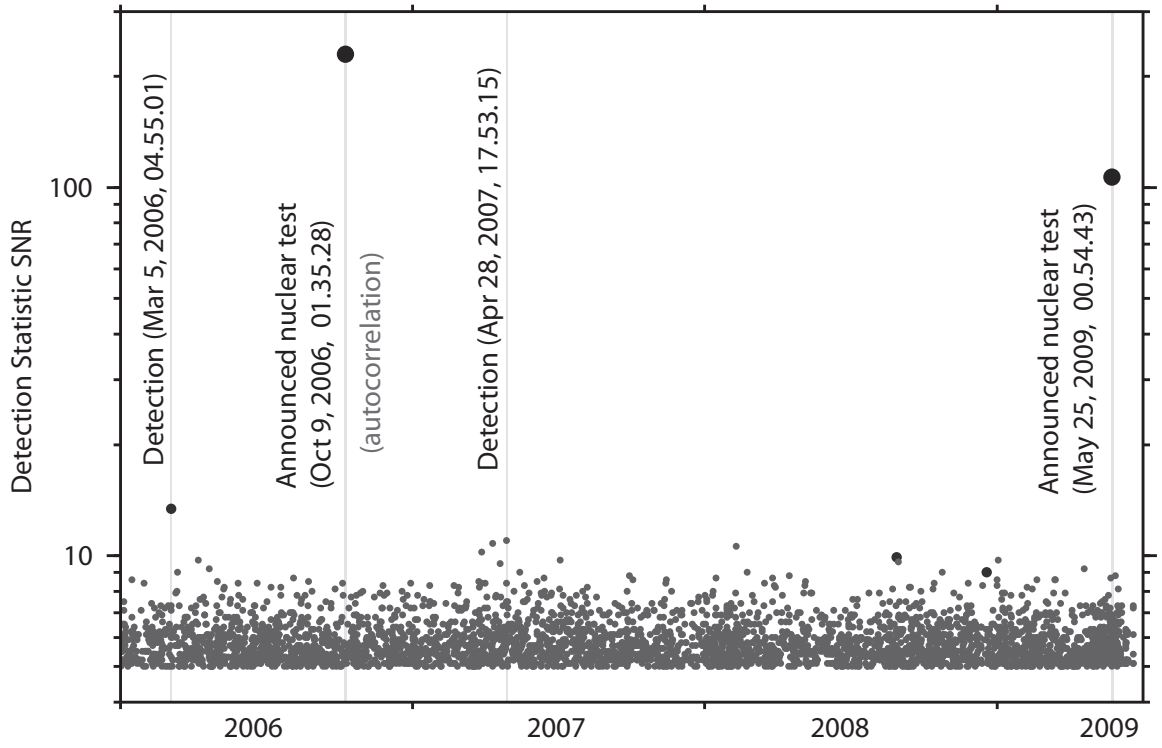

Fig. 6.2.4. Detections from the correlator on the MJAR array where the 8 second long signal template begins at a time 2006-282:01.37.32.6. The value denoted "Detection statistic SNR" is described in the text and measures the ratio between the array detection statistic C(t), defined in Equation 6.2.3, and the background level of the same quantity. Vertical bars indicate the times of the four highest values obtained in the period January 1, 2006, to June 20, 2009. The symbol size is proportional to the log of the array detection statistic.

Waveform similarity will be reduced with decreasing size of a subsequent nuclear test. This will be partly due to a decreased SNR, given a generated signal with smaller amplitude, but may also result from rather different spectral characteristics of the generated signal. There is however reason to suppose that, for this magnitude of event, within the frequency band chosen here, that there is not likely to be great variation in the signal. Gibbons et al. (2007) took a signal from a magnitude 3.5 earthquake and, using the same multi-channel procedure on the NORSAR array, successfully detected almost co-located events down to magnitude 0.5. It is likely that the greatest contribution to waveform dissimilarity will come from distance of the source location from the hypocenter of the template event.

We need in any case to set the detection threshold low enough as to allow for as great a departure as possible from the master event waveforms while keeping the false alarm rate at a minimum. Figure 6.2.4 and Table 6.2.1 provide an informative means of determining which threshold should be considered for reexamining detected signals. Selecting only the occasions where the array detection statistic exceeds the standard deviation by a factor of 10 results in only seven detections throughout the entire test period. Given the sharp increase in the number of detections at lower thresholds, 10 was determined to be a useful working SNR threshold.

6.2.3 Eliminating and Examining False Alarms

The first comment on the occurrence of false alarms is to stress the importance of the f-k post-processing. Figure 6.2.5 indicates, for intervals of the array detection statistic, the number of detections obtained both with and without the automatic screening of detections which fail to meet the requirements of the f-k post-processing algorithm. Without this waveform-alignment test, 2496 as opposed to 7 detections would have been registered over the provisional threshold SNR of 10 in the test period. This clearly constitutes a dramatic reduction in the human resources necessary to evaluate the detector output.

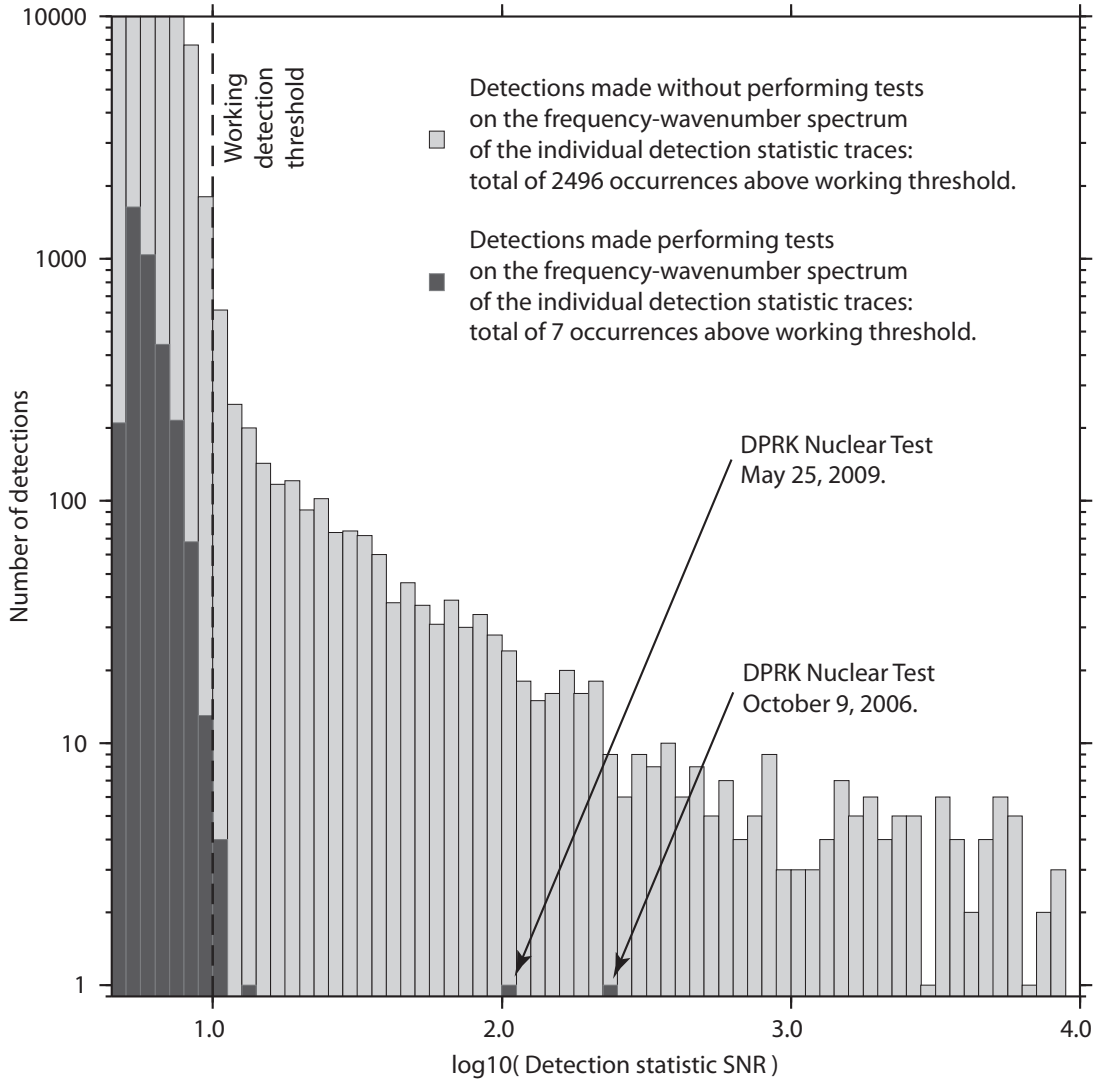

Fig. 6.2.5. Histograms of correlation detections with and without f-k post-processing on the individual channel detection statistic traces. The number of detections in each bin corresponds to the time-interval displayed in Figure 6.2.4.

Many of the detections at the lower SNR end of the spectrum are indeed caused by seismic background noise and wavefronts arriving from somewhat different directions. At the higher SNR end of the spectrum, the detections which are eliminated by the f-k post-processing are almost exclusively the result of faults in the data: e.g. gaps and spikes. A data discontinuity will frequently either affect one channel only or will affect all channels simultaneously. The multi-

channel waveform template has encoded an intrinsic time-dependence which is only likely to produce aligned correlation coefficient traces if the incoming wavefield encodes the same time-dependence. It is of course frequently possible to exclude such false alarms by other quality control methods. However, the simplicity of the f-k post-processing method, coupled with its ability to screen a full spectrum of false alarms, makes it both a robust and effective method of online, automatic quality control.

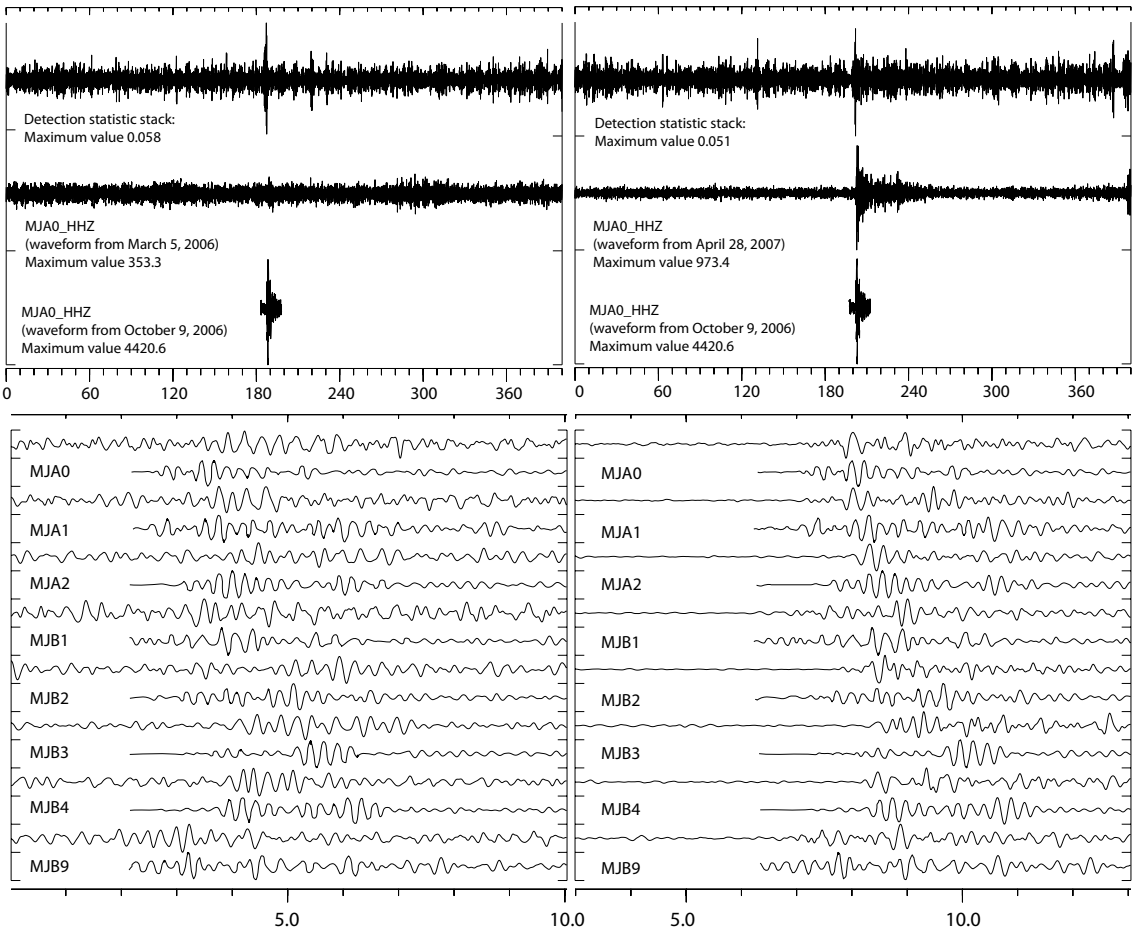

Fig. 6.2.6. Waveforms and detection statistic stack traces for the two correlation detections with the highest values of the detection statistic SNR (the announced nuclear tests excluded). In each waveform couplet, the lowermost trace is the template from the 2006 DPRK nuclear test signal.

Of the small number of detections which both exceeded the nominal detection threshold and which passed the f-k post-processing tests, the two "best" detections are displayed in Figure 6.2.6. In the right hand panel, the correlation detection clearly corresponds to a phase arrival which can be associated with an event in the bulletin of the International Seismological Center (ISC, http://www.isc.ac.uk/) with origin time, latitude and longitude 2007-118:17.54.52.3, 37.45 degrees N, 136.46 degrees E. The location of this event is shown in the map in Figure 6.2.7 and clearly falls almost on the great circle path to the North Korea test site. The implication of this is that while the source type and location of the events were very different, the fact that the resulting wavefront has propagated through the rock close to the array in almost the same direction as the wavefront from the nuclear test, both the correlation and the alignment of waveforms was sufficiently good to result in a detection.

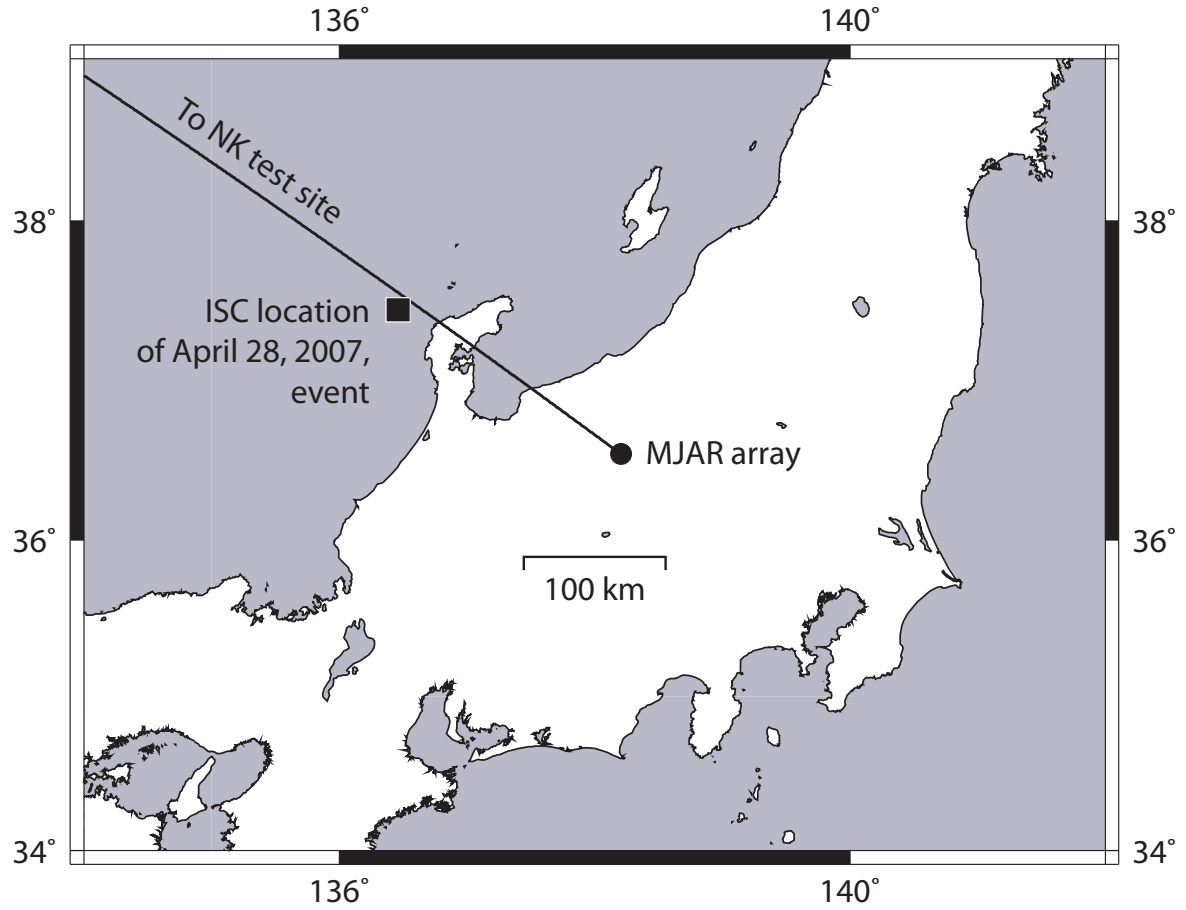

Fig. 6.2.7. ISC location of the April 28, 2007, event relative to the MJAR array.

The detection displayed in the left hand panel of Figure 6.2.6 does not appear to result from a visible signal, and no event is present in the ISC bulletin which could have generated a signal at this time and place. The segment of data which correlates best with the template starting at time 2006-282:01.37.34.0 begins at a time 2006-064:04.57.07.4. Data from the INCN and MDJ stations were obtained from the IRIS DMC for this time period and no evidence was observed in these waveforms for an event close to the test-site.

6.2.4 Examining the Detection Threshold

It is of great interest to examine how effective the correlation procedure is at detecting copies of the signals from the two announced nuclear tests, scaled down and submerged into background noise on the MJAR array. The experiment is designed to examine the magnitudes down to which events will be detected reliably using the correlation procedure. No spectral rescaling is applied to the data; we defend a linear scaling of filtered waveforms by referring to the results of Gibbons et al. (2007). Two different experiments were carried out. In the first, copies of the signal from the 2006 test were scaled down into background noise and, in the second, copies of the signal from the 2009 test were used. In all cases, the waveform template used for the matched filter was the signal from the 2006 test. Both experiments were essentially a repeat of the standard detection run described above, except that for every 20 minute long segment of data, a scaling factor between 0.0001 and 1.0 was selected (pseudo-randomly) and a copy of

the signal of interest was submerged into the data with this scaling. The results of this study are displayed in Figure 6.2.8, where the scaling factor applied has been converted to an indication of the inferred event magnitude as shown.

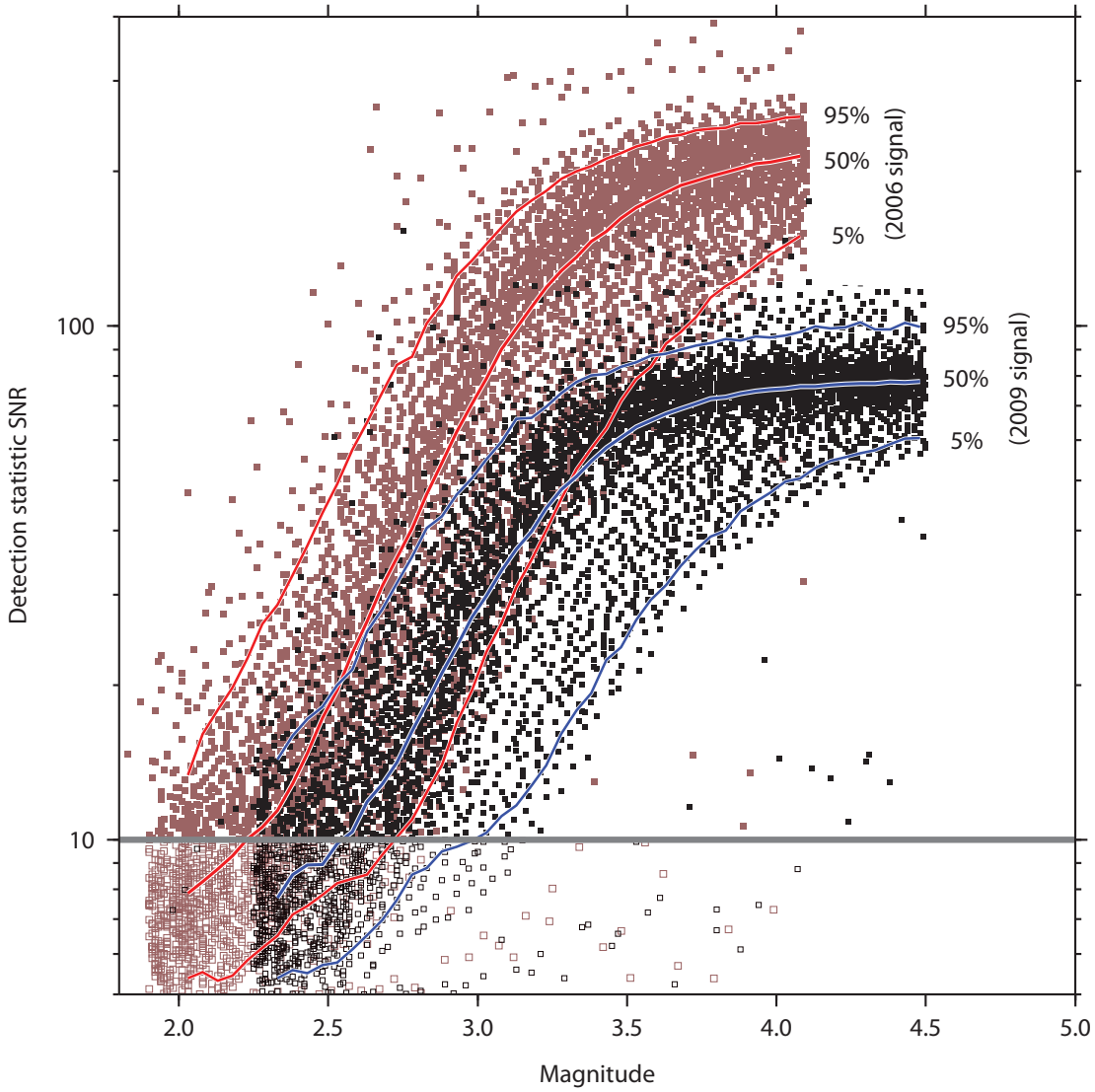

Fig. 6.2.8. Detectability using a multi-channel correlator on the MJAR array of signals from the 2006 and 2009 explosions, scaled down into different segments of background noise, using the signal from the 2006 explosion as a template. The mb magnitudes for the 2006 and 2009 events are assumed to be 4.1 and 4.5 respectively and the magnitude of the simulated events are taken to be 4.1 + log10(epsilon) and 4.5 + log10(epsilon) where epsilon is the factor that the explosion signal is scaled by before adding to the background noise at a given time. Only one in 50 of the points used to estimate the detectability curves is plotted on the graph. The detectability curves are based on the points contained in intervals of 0.05 magnitude units.

Figure 6.2.8 displays the detection statistic SNR, of which there is clearly a large spread for any given scaling factor. The time-period explored lasts from January 1, 2006, to June 20, 2009, and - considering that one submerged signal was added to the data every 20 minutes during this period - we cover every eventuality of background noise level, including the codas of large earthquakes.

The detection statistic SNR for the scaled-down copies of the 2006 signal decrease almost immediately as the magnitudes of the simulated events decrease. The values of the detection statistic SNR for the scaled down copies of the 2009 signal start at a lower level than for the 2006 signal (since the signals do have a slightly different form to the detection template) but are not affected greatly by applying a scaling factor between 0.1 and 1.0 (probably due to the large SNR of the 2009 signal). Down to a simulated magnitude of ~2.7, 95% of the submerged 2006-signals are still recording values of the detection statistic SNR above the nominal threshold of 10.0. The same is true for simulated copies of the 2009 event down to magnitudes of ~3.0. 50% of the 2009 signals scaled down to magnitude ~2.6 are being detected as are 50% of the 2006 signals scaled down to magnitude ~2.3.

6.2.5 Summary

We have demonstrated that performing multi-channel cross-correlation on the MJAR array in Japan, with a signal template taken from the October 9, 2006, North Korea nuclear test, is able to detect the signals from the May 25, 2009, North Korea test with a very low false alarm rate. Crucial to the low false alarm rate in this study is the performing of f-k analysis on the individual sensor detection statistic traces which eliminates false alarms both due to unrelated seismic signals and problems in the data.

A scaling study, whereby signals from both 2006 and 2009 tests are scaled down and submerged into the background noise, suggests that, at a detection threshold which results in a negligible number of detections, events down to magnitude ~3.0 at the site of the 2009 test are detected by the correlation procedure in 95% of cases.

It is pointed out that this study used only data from the MJAR array (Matsushiro, Japan) which, due to problems of signal incoherence at high frequencies, was unable to contribute to the automatic event location estimate for either 2006 or 2009 DPRK nuclear tests. The multi-channel correlation procedure demonstrated here is insensitive to waveform incoherence between sensors and can be used to detect signals from new events if we have a template signal from an event close-by. This is the case for the DPRK test site and many other sources of both natural and anthropogenic seismicity. Large scale correlation detectors in operational pipelines are to be advocated for automatic signal detection and event classification.

Acknowledgements

Data from the MJAR array was obtained via the IDC in Vienna, Austria.
Data from the MDJ station was obtained via the IRIS DMC and is made available via the IC network. Data from the INCN station was obtained via the IRIS DMC and is made available via the IU network.

All maps were generated using GMT software (Wessel and Smith, 1995).

References

Capon, J. (1969). High-Resolution Frequency-Wavenumber Spectrum Analysis, *Proc. IEEE*, **57**, 1408-1418.

Gibbons, S. J. and Ringdal, F. (2006). The detection of low magnitude seismic events using array-based waveform correlation, *Geophys. J. Inter.*, **165**, 149-166.

Gibbons, S. J., Ringdal, F., and Kværna, T. (2008). Detection and Characterization of Seismic Phases Using Continuous Spectral Estimation on Incoherent and Partially Coherent Arrays, *Geophys. J. Inter.*, **172**, 405-421.

Gibbons, S. J., Bøttger-Sørensen, M., Harris, D. B., and Ringdal, F. (2007). The detection and location of low magnitude earthquakes in northern Norway using multi-channel waveform correlation at regional distances, *Phys. Earth Planet. Inter.*, **160**, 285-309.

Gibbons, S. J. and Ringdal, F. (2010). Detection and Analysis of Near-Surface Explosions on the Kola Peninsula, *Pure Appl. Geophys.*, **167**, 413-436.

Kato, M., Nakanishi, I., and Takayama, H. (2005). Variation of teleseismic short-period waveforms at Matsushiro Seismic Array System, *Earth, Planets, Space*, **57**, 563-570.

Kennett, B. L. N. (2002). *The Seismic Wavefield. Volume II: Interpretation of Seismograms on Regional and Global Scales*, Cambridge University Press, Cambridge, UK. ISBN 0 521 00665 1.

Kværna, T., Ringdal, F., and Baadshaug, U. (2007). North Korea's Nuclear Test: The Capability for Seismic Monitoring of the North Korean Test Site, *Seism. Res. Lett.*, **78**, 487-497.

Selby, N. D. (2010). Relative locations of the October 2006 and May 2009 DPRK announced nuclear tests using International Monitoring System seismic arrays, *Bull. Seism. Soc. Am.*, **100**, 1779-1784.

Shelly, D. P., Beroza, G. C., and Ide, S. (2007). Non-volcanic tremor and low-frequency earthquake swarms, *Nature*, **446**, 305-307.

Wen, L., and Long, H. (2010). High-precision Location of North Korea's 2009 Nuclear Test, *Seism. Res. Lett.*, **81**, 26-29.

Wessel, P. and Smith, W. H. F. (1995). New version of the Generic Mapping Tools, *EOS Transactions of the American Geophysical Union*, **76**, 329.

S. J. Gibbons

6.3 A probabilistic seismic model for the European Arctic

Sponsored by the National Nuclear Security Administration

Award Nos: DE-AC52-08NA28651(NORSAR,UiO) and LL08-BAA08-38-NDD03 (LLNL)

6.3.1 Introduction

The area of interest for this study is the European Arctic, in particular the Barents Sea and surrounding regions such as the Norwegian-Greenland Sea, the Southern Eurasian Basin, Novaya Zemlya, the Kara Sea, the East European Lowlands, the Kola Peninsula and the Arctic plate boundary (Figure 6.3.1).When developing a seismic model the focus is often on finding one single best fitting model. Existing models for the region are based on approaches that try to find the model with the best fit to one or several dataset. The resulting models contain little to no information about model uncertainties. Knowledge about the robustness of features in seismic models is however beneficial for the geological interpretation of models and the reliable determination of location uncertainties for seismic events.

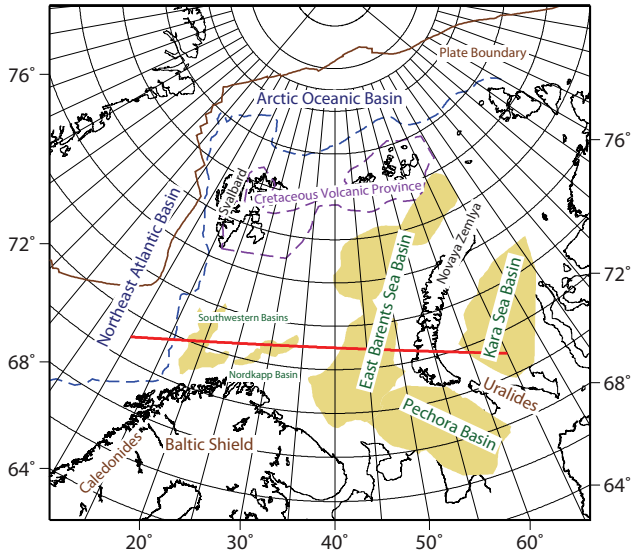

Fig. 6.3.1. Simplified tectonic map of the region after Ritzmann et al. (2007) and Bird (2003). The plate boundary is given by the brown line and continent-ocean boundary by the dashed blue line. Beige areas represent the major sedimentary basins in the Region. The cross-section along which we will examine our probabilistic model in Figure 6.3.3 is outlined in red.

Our probabilistic model differs from traditional seismic models in that it describes the posterior distribution, the ensemble of models which fit the data. The posterior distribution is proportional to the product of the prior distribution and the likelihood function. The prior distribution represents the ensemble of plausible models and the likelihood function makes models with a good fit to the data more likely than models with bad fit to the data. The data we use are thickness constraints, velocity profiles, gravity data, surface wave group velocities and body wave travel times. In this work a Markov Chain Monte Carlo (MCMC) technique is used to sample the unknown posterior distribution. This process results in 4,000 models that all fit the data.Analyzing this ensemble of models that fit the data allows to estimate a mean model and the standard deviation for the model parameters, i.e. their uncertainty. Maps of sediment thickness and thickness of the crystalline crust derived from the posterior distribution are in good agreement with knowledge of the regional tectonic setting. The predicted uncertainties, which

are equally important as the absolute values, correlate well with the variation in data coverage and data quality in the region. In addition to this a probabilistic model allows the formulation of seismic event location techniques that take into account uncertainties in the velocity model.

6.3.2 Probabilistic model

We determined an average model to compare the results of this study to other studies of the same region. The real power of a probabilistic model lies however in the fact that it describes the distribution of models that fit the data, as we will see later in the location example.

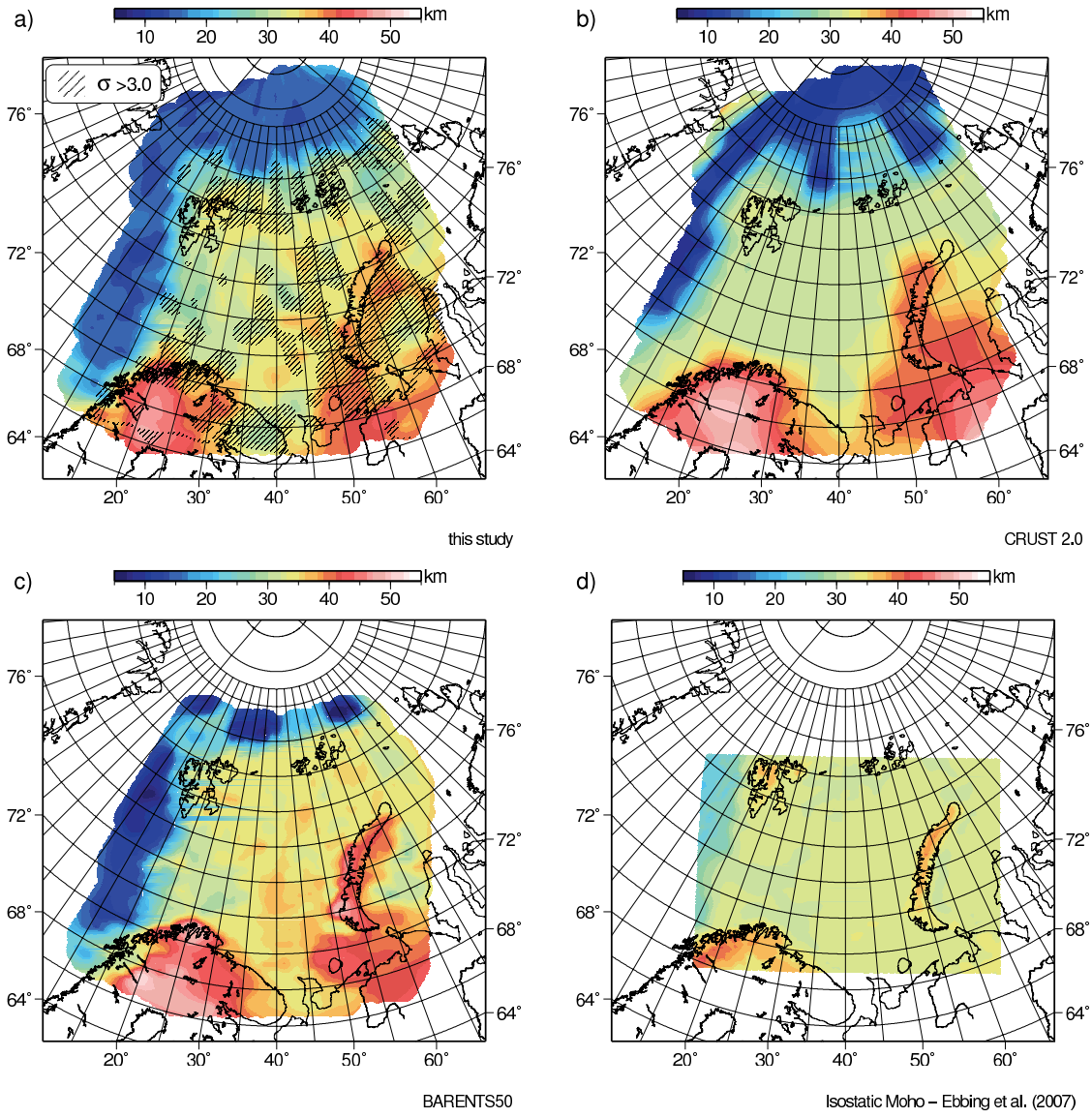

Fig. 6.3.2. Depth to Moho: a) Mean model obtained in this study, b) CRUST 2.0 after Bassin et al. (2000), c) BARENTS50 after Ritzmann et al. (2007) and d) isostatic Moho of Ebbing et al. (2007).

Figure 6.3.2 shows the depth to Moho in this study, CRUST 2.0 (Bassin et al., 2000), BARENTS50 (Ritzmann et al.,2007) and for an isostatic Moho computed by Ebbing et al. (2007). It is important to keep in mind that the different models have different spatial resolu-

tions; our model for example has a node spacing of 83 km while CRUST 2.0 uses a 2 by 2 degree grid. This makes it necessary to resample the models for this comparison. Unlike the other models our probabilistic model also provides estimates for the uncertainties, thus we can compute a standard deviation in addition to the mean of our samples of the posterior distribution. We have hatched the areas where the standard deviation on the Moho exceeds 3 km, indicating where this parameter is poorly constrained. The models are generally similar, with some notable differences. For example, most models see more complexity within the major tectonic provinces than the relative simple CRUST 2.0 model. Also, the Moho recovered by BARENTS50 appears more detailed than the Moho recovered in the present study. This comes as no surprise when one takes into account that BARENTS50 has a spatial resolution of 50 km. The models differ the most from each other around Novaya Zemlya and in the Kara Sea. Interestingly this is also where the uncertainties in the depth to Moho are generally larger than 3 km in our study. The isostatic modeling of Ebbing et al. (2007) suggests, as expected, a shallower and smoother Moho than the other, seismically-based models.

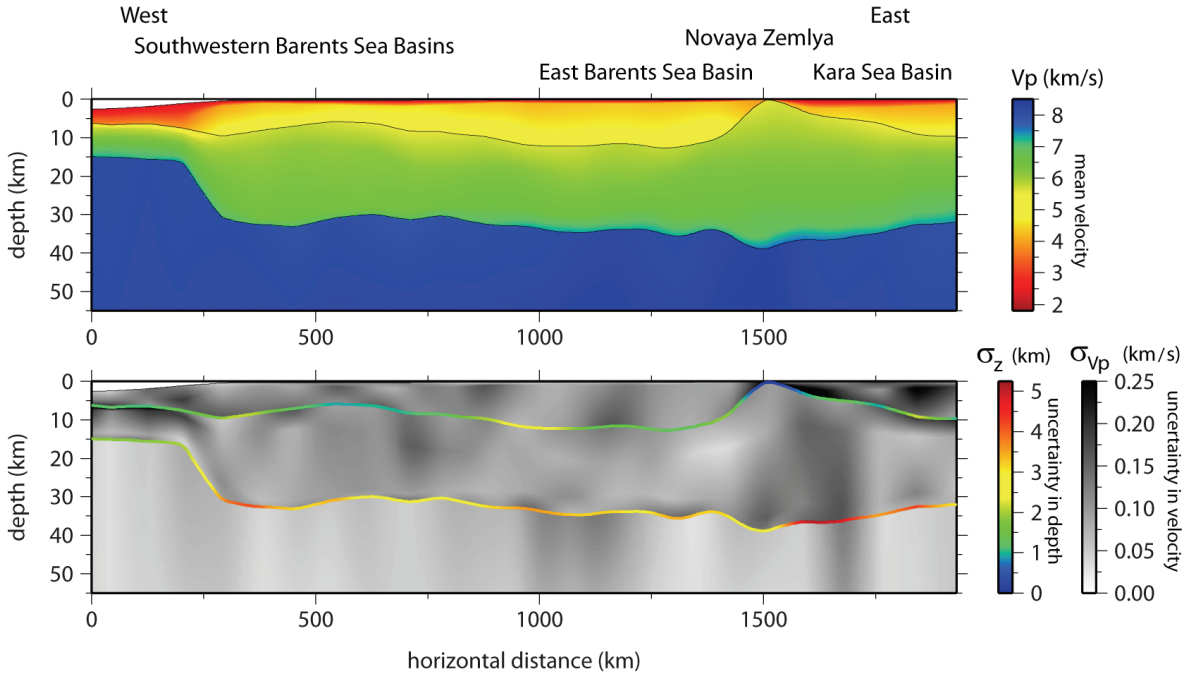

Fig. 6.3.3. West-east cross-section along the great circle path shown in Figure 6.3.1; the top panel shows Vp and the bottom panel shows the uncertainty in Vp. In the bottom panel interfaces are colored according to the uncertainty in depth.

Figure 6.3.3 shows a west to east cross-section through our probabilistic model. Unlike cross-sections further north across the western continental margin, we find a relatively rapid transition in crustal thickness and see an increase in crustal thickness associated with Novaya Zemlya. The highest uncertainty in depth to Moho lies below the Kara Sea. This is related to the weak constraints on the Moho here: gravity data and a velocity profile with a relatively high uncertainty, with no body waves sampling the Moho. We clearly recover the East Barents Sea and Kara Sea basin. The sedimentary basins in the southwestern Barents Sea, on the other hand, are only tens of kilometers wide. The node spacing of 83 km used in this study means that we cannot recover these basins. What we are able to recover is the fact that the sedimentary layer is on average thicker if there are several sedimentary basins a few tens of kilometers wide.

The sediments on the epicontinental Barents Shelf have significantly higher velocities than sediments covering the oceanic crust. This feature of our model can be linked to the uplift of the region in the Neogene and the repeated phases of glaciation in the Barents Sea during the late Pliocene and Pleistocene (Smelror et al., 2009). Uplift and glaciation cause erosion of the sediments covering the Barents Shelf and the deposition of large amounts of young sediments into major submarine fans along the western and northern margin. These young sediments are less consolidated and have as a consequence lower seismic velocities when compared to the older sediments covering the Barents Shelf. The uppermost sediments in the Kara Sea Basin show slightly lower velocities than the uppermost sediments in the East Barents Sea Basin. This correlates with the interpretation that only during the maximum extent of glaciation in the late Pleistocene did the ice sheet reach into the Kara Sea (Smelror et al., 2009). Sediments in the Kara Sea have therefore experienced less erosion, leaving less compacted sediments exposed at the seafloor, possibly together with deposits from other periods of glaciation

6.3.3 Probabilistic earthquake location

The non-linear problem of seismic event location using body wave travel times is often solved using non-linear iterative approaches. A poor station distribution and a complex 3D velocity structure however contribute to the non-linearity of the location problem and create potential instabilities. The potential failure of linearization together with the need for more comprehensive location uncertainty information in the form of a probability density function has led to the formulation of numerous probabilistic approaches (e.g. Kennett and Sambridge, 1992; Billings, 1994; Lomax et al., 2000). Location uncertainty is caused by pick uncertainties (i.e., the inability to accurately estimate onset time for a phase) and uncertainties in the velocity models. Most estimates for location uncertainty do not however take into account the uncertainties in the model used to predict the travel times. They are solely based on pick uncertainties. A probabilistic model, on the other hand, allows a prediction of observables and their uncertainties.

The distribution of an observable (i.e., its value and uncertainty) given a probabilistic model can be recovered by calculating its values for every model belonging to the set of samples that defines the probabilistic model. Similarly it is possible to obtain an estimate for the location uncertainty of a seismic event due to model uncertainty by locating the event for all the models that comprise the posterior set. Here we use an MCMC approach to approximate the posterior distribution for the origin time and location of an earthquake. The maximum of the posterior distribution then defines the hypocenter location and origin time.

We use an earthquake in the western Barents Sea to investigate the influence of model uncertainties on location uncertainties. Figure 6.3.4.a shows the station distribution, and Figure 6.3.4.b the distribution of the mean path velocities, between the event and two selected stations. For longer paths which reside primarily in the mantle, the mean velocity is less influenced than for shorter paths that reside in the crust. We have located the earthquake for each of the models in the posterior distribution. Figure 6.3.4.c shows the 4,000 locations obtained and thereby provides an estimate for the location uncertainty from model errors alone together with an event location obtained using a regional 1D velocity model. All stations available for the location of this event lie to the west of the earthquake. This results in both the error ellipse for the 1D velocity model solution and the cloud of locations being elongated in the west-east direction. We observe a linear trend between late deep event locations to the southwest and early shallow locations to the northeast. Bondár et al. (2004) showed that for an excellent station coverage, depth and origin time are more sensitive to the velocity model than the epicenter

location. We find that for an uneven station distribution as shown here the epicenter location seems to be equally sensitive to the velocity model as to the origin time and depth.

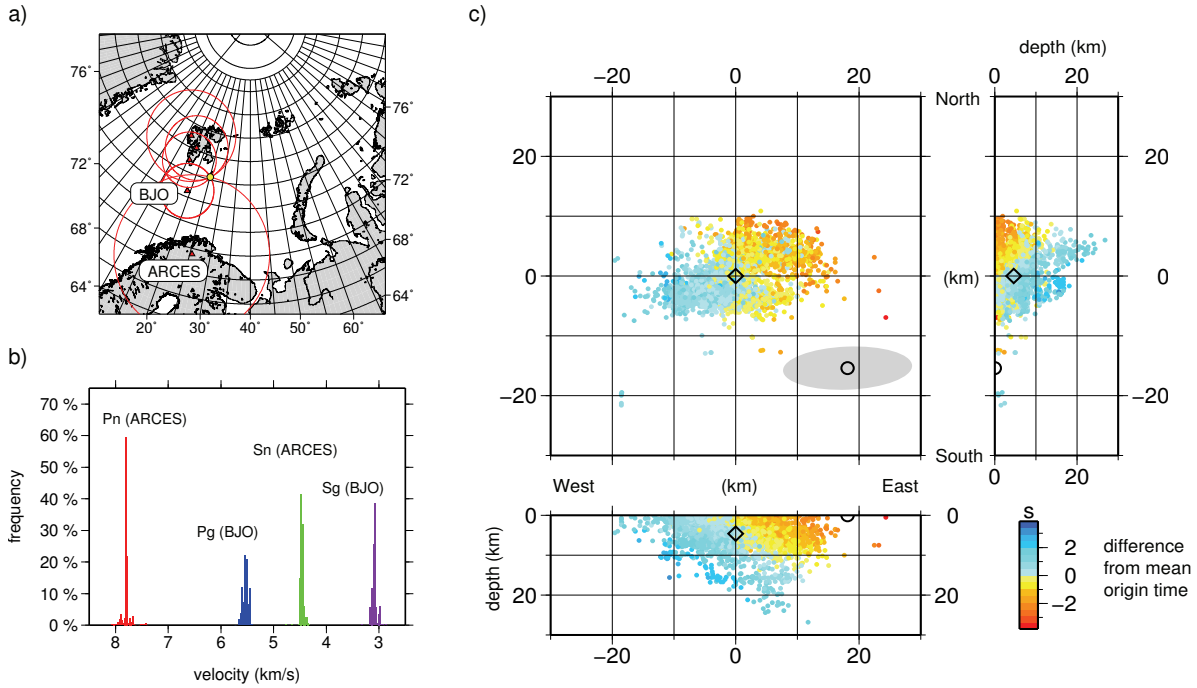

Fig. 6.3.4. Probabilistic location of an earthquake, taking model uncertainties into account: a) station distribution, b) distribution of average path velocities for regional phases for two stations used in the location example and c) hypocenter and origin time of the earthquake computed for each of the models forming our probabilistic model. The mean location is given by the black diamond. The points are colored according to the deviation from the mean origin time of our set of locations. The black circle marks the location of the event computed using a 1D velocity model and a fixed depth of 0 km and the error ellipse is given by the gray shaded area.

6.3.4 Concluding remarks

We have successfully employed a probabilistic approach for the development of a data-driven regional seismic model for the European Arctic. We have compared the mean model of our posterior distribution with other models that cover the region and find that it captures the features that can be resolved with a node spacing of 83 km. Our probabilistic model not only provides images of the subsurface together with estimates of uncertainties, it also allows for the prediction of observables and uncertainties. This can be used to derive seismic event location uncertainties from model uncertainties and can in the future be used for location algorithms that take model uncertainties in addition to uncertainties in onset time into account.

Acknowledgements

We thank NOTUR (The Norwegian Metacenter for Computational Science) and the University of Oslo for providing the computational resource on the Titan III high performance computing facilities. We thank Stephen Myers (LLNL) for contributing the ground Truth data and NGU (The Geological Survey of Norway) for providing the depth to Moho data shown in Figure 6.3.2.d.

Juerg Hauser, NORSAR
Kathleen M. Dyer, LLNL
Michael E. Pasyanos, LLNL
Hilmar Bungum, NORSAR
Jan Inge Faleide, UiO
Stephen A. Clark, UiO
Johannes Schweitzer, NORSAR

References

Bassin, C., G. Laske, and G. Masters (2000). The current limits of resolution for surface wave tomography in North America, EOS Trans. AGU, **81**, F897.

Billings, S. (1994). Simulated annealing for earthquake location, Geophys. J. Int., **118** (3), 680-692.

Bird, P. (2003). An updated digital model of plate boundaries, Geochem. Geophys. Geosyst., **4** (3), 1027.

Bondár, I., S. Myers, E. Engdahl, and E. Bergman (2004). Epicentre accuracy based on seismic network criteria, Geophys. J. Int., **156** (3),483-496.

Ebbing, J., C. Braitenberg and S. Wienecke (2007). Insights into the lithospheric structure and the tectonic setting of the Barents Sea region by isostatic considerations, Geophys. J. Int., **171**, 1390-1403.

Kennett, B. L. N. and M. Sambridge (1992). Earthquake location - genetic algorithms for teleseismic location, Phys.Earth Planet. Inter., **75** (1-3), 103-110.

Lomax, A., J. Virieux, P. Volant, and C. Berge (2000). Probabilistic earthquake location in 3D and layered models: Advances in Seismic Event Location, pp. 101-134.

Ritzmann, O., N. Maercklin, J. I. Faleide, H. Bungum, W. D. Mooney and S. T. Detweiler (2007). A 3D geophysical model for the crust in the greater Barents Sea region: Model construction and basement characterization. Geophys. J. Int., **170,** 417-435.

Smelror, M. O., O. Petrov, G. B. Larsen and S.Werner (2009). Geological History of the Barents Sea, Geological Survey of Norway.

6.4 Local seismicity on and near Bear Island (Norwegian Arctic) from a temporary small aperture array installation in 2008

6.4.1 Introduction

As part of the International Polar Year project (IPY) "The dynamic continental margin between the Mid-Atlantic-Ridge system (Mohns Ridge, Knipovich Ridge) and the Bear Island region", a temporary small aperture array was installed on Bear Island (Bjørnøya) during the summer of 2008. The aim of this project was to improve the understanding of the structure, the stress conditions and sources, the dynamics of the continental margin, and to identify active tectonic structures (Schweitzer et al., 2008). Seismicity in the region has been studied with a virtual seismic network comprising the existing permanent stations in the region, the Bjørnøya array, 12 ocean bottom seismometers, and two new broadband seismometers on Svalbard (Hornsund) and Hopen. The network detected large numbers of events along the Mohns and Knipovich ridges and the Senja Fracture Zone, as well as an M=6 event near Svalbard in February 2008 which was followed by an extensive aftershock sequence.

It became clear that the vast majority of the seismic signals recorded at the Bear Island array correspond to relatively local sources. Some of these local sources are likely to be due to human activity at the meteorological station in the northern part of Bear Island, although many are likely to be caused by weather-related phenomena: the melting of snow or the drifting and breaking of ice floes on the rivers and lakes on Bear Island. Rockfall along the steep coastal line or in the mountainous southern part of the island would be another plausible explanation. Tectonic events on or near the island would be of great interest.

Within the framework of a research visit at NORSAR in March and April 2010, financed by the EC Project NERIES (http://www.neries-eu.org/), this study aimed to investigate local events on and around Bear Island. It was assumed that events caused by weather-related phenomena could be identified by finding correspondence between event occurrence and meteorological data.

6.4.2 Array constellation and data processing

The position of Bear Island on the Barents Sea Shelf is shown in Fig. 6.4.1. It is situated half-way between the northern tip of Norway and Svalbard. The array was operative from May 22 to September 29, 2008. It consisted of 13 3-component stations of the type LE3D5s, with a corner frequency of 5 seconds, deployed over an aperture of 5-7 kilometer in the northern and central part of the island (Fig. 6.4.2). Additionally, data from the permanent broadband station BJO1 near the meteorological station were available.

The array was used as a network to localize events with clear body wave onsets, by applying the NORSAR HYPOSAT software (Schweitzer, 2001; 2002). For this purpose an underground model for P-wave velocities was available from reflection and refraction seismic experiments carried out within the framework of the IPY project (Czuba et al., 2010). Since it was not possible to establish an additional model for shear wave velocities by analyzing surface wave dispersion curves of regional events or ambient noise analysis (Wathelet et al., 2008; Endrun et al., 2009), an ideal P- to S-wave velocity ratio of $\sqrt{3}$ was assumed. The velocity of Rayleigh waves could be estimated through array techniques like beamforming and f-k-analysis.

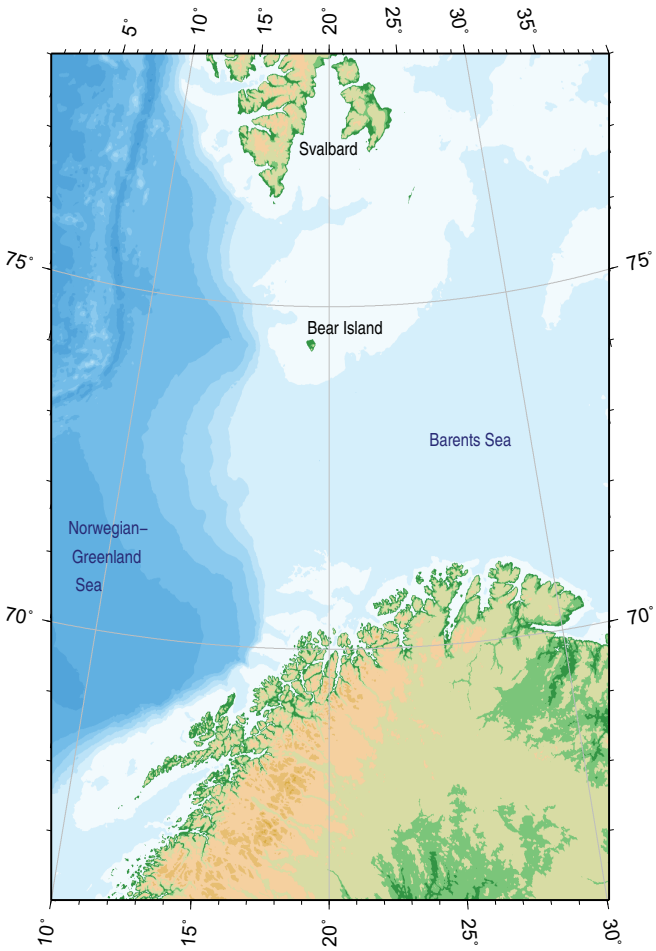

Fig. 6.4.1. Map of the Norwegian-Greenland Sea and the Norwegian continental margin between Fennoscandia and the Svalbard Archipelago (from: The GEBCO_08 Grid, version 20091120, http://www.gebco.net).

The NORSAR processing software for seismic data was applied to data from the Bear Island array. It provided continuous estimates of apparent velocity and backazimuth for arriving signals throughout the whole period of operation. From this processing, different events where located and their locations could be used in this seismicity study.

A waveform correlation detector (Gibbons & Ringdal, 2006) was applied to a number of observed signals in order to identify sources of recurring seismicity. The resulting temporal distributions of some events were compared with weather and climate data supplied by the Norwegian Meteorological Institute via its web site (http://eKlima.met.no). Values of wind direction, wind speed and temperature were available hourly from the weather station on Bear Island, as were values for wave height (every three hours), snow cover (daily) and type and amount of precipitation (daily).

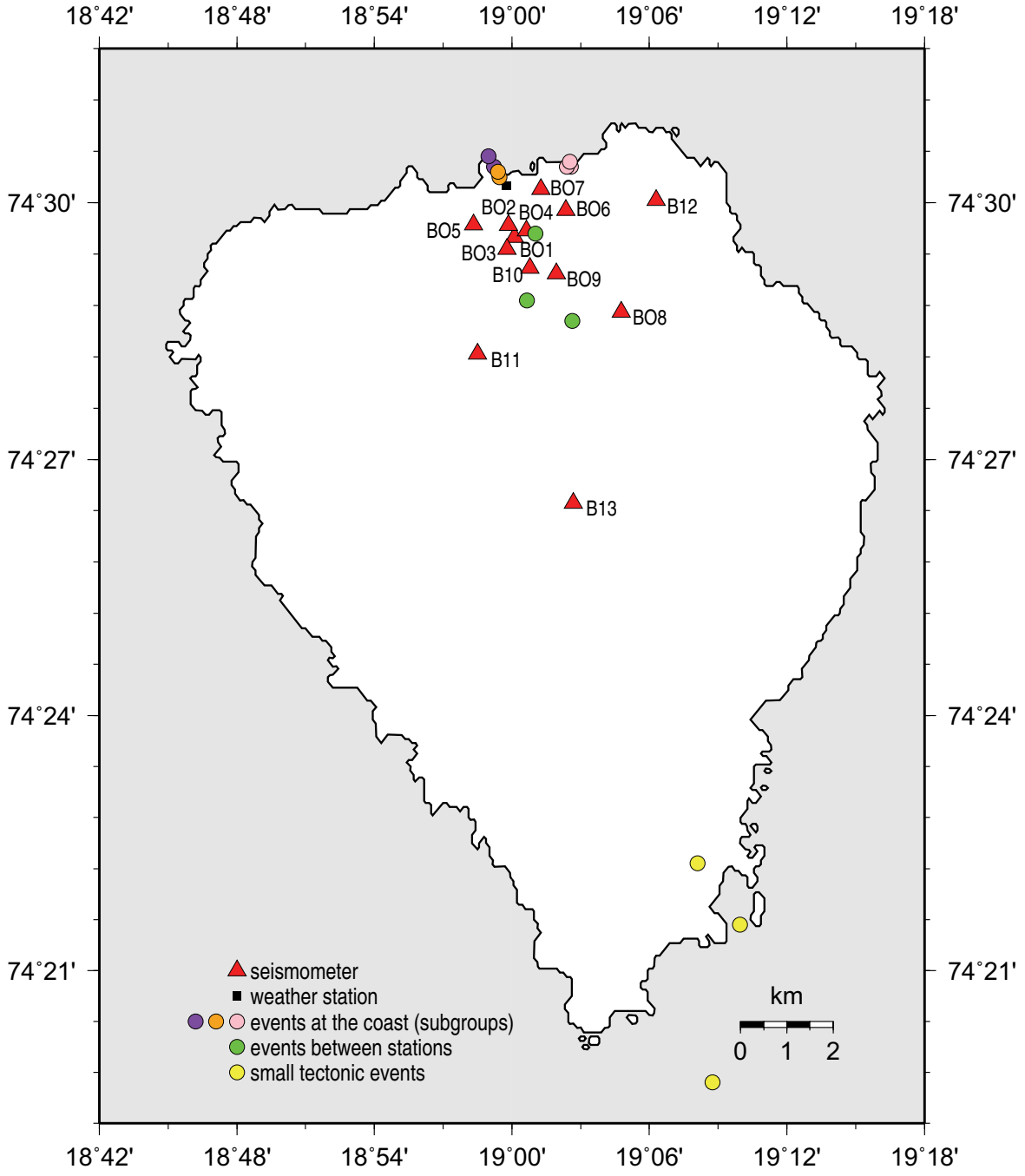

Fig. 6.4.2. Station map of the temporary small aperture array on Bear Island in 2008. The positions of localized events are marked by colored dots, the black square shows the position of the weather station.

6.4.3 Different event groups

In the course of the survey, three major groups of events could be identified and located. The first group can most likely be associated with weather and wave phenomena at the northern coast. A second group consists of events located within or close to the array and which are assumed to correspond to melting snow and breaking of ice floes on the rivers and lakes of the island. The third and probably most interesting group consists of small tectonic events on and near Bear Island. All manual event location estimates are shown in Fig. 6.4.2. A fourth set of observations consists of small acoustic signals, which were detected on several occasions. No event location estimate was possible for these signals since the observations in each case comprised only a single acoustic signal arriving at the array as plane waves from the south west. They are most likely to be associated with ships passing the island.

Events at the northern coast

The vast majority of all detected signals are associated with events located at the northern coast of the island (northcoast events). The signals are just one second long and are primarily recorded at the northernmost stations of the array. The amplitude quickly decreases so that the signals can not be observed at the inland stations. Body- and clear surface-waves arrive with very shallow incidence angles at the seismic stations. The primary onset is dominant on the horizontal components, indicating shallow events nearby. An example for such a signal is shown in Fig. 6.4.3.

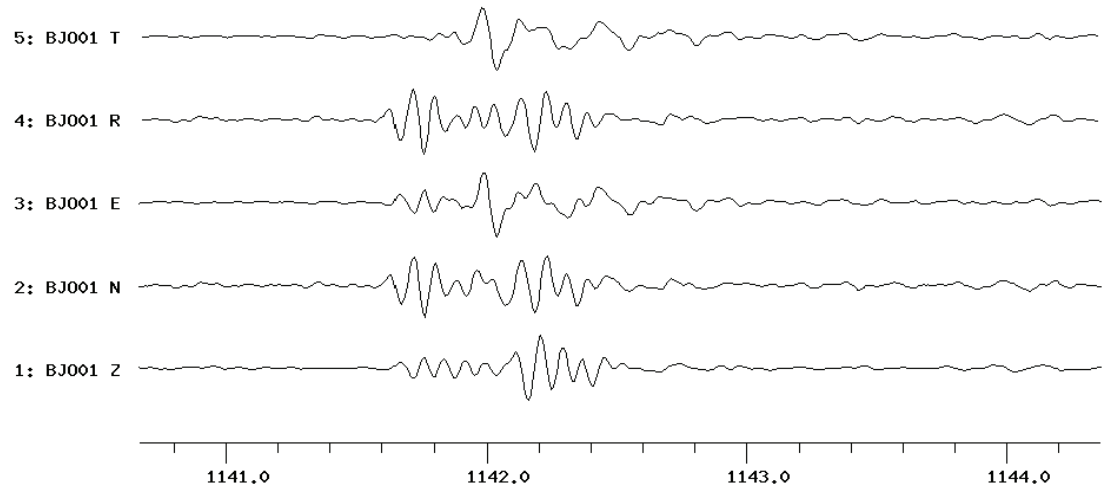

Fig. 6.4.3. Northcoast event from June 1, 2008 recorded at station BJO01. The traces are rotated with a backazimuth of 339° and filtered with a Butterworth bandpass filter from 3-16 Hz. The time axis shows seconds since midnight.

The temporal distribution of the events was determined by waveform correlation and is clearly inhomogeneous (Fig. 6.4.4). No periodicity can be observed. Three subgroups of events could be identified based on differences in their frequency content, their occurrence in time and space and the kind of phases that arrive. The major subgroup consists of about 80,000 events, (purple dots in Fig. 6.4.2) the other two subgroups contain “only” 22,000 (orange dots in Fig. 6.4.2)

and 14,000 events (pink dots in Fig. 6.4.2), respectively.
An emphasis in the analysis was put on the subgroup with the most detected events.

Human activity at the meteorological station can be eliminated as a possible source of these events. The origins do not coincide with the location of the weather station and there is no characteristic day and night cycle that one would assume in connection with human activity. No correlation with temperature and snow melting could be observed so that intensified erosion at the coast, either due to thawing of the permafrost or snow water, can be excluded as well.

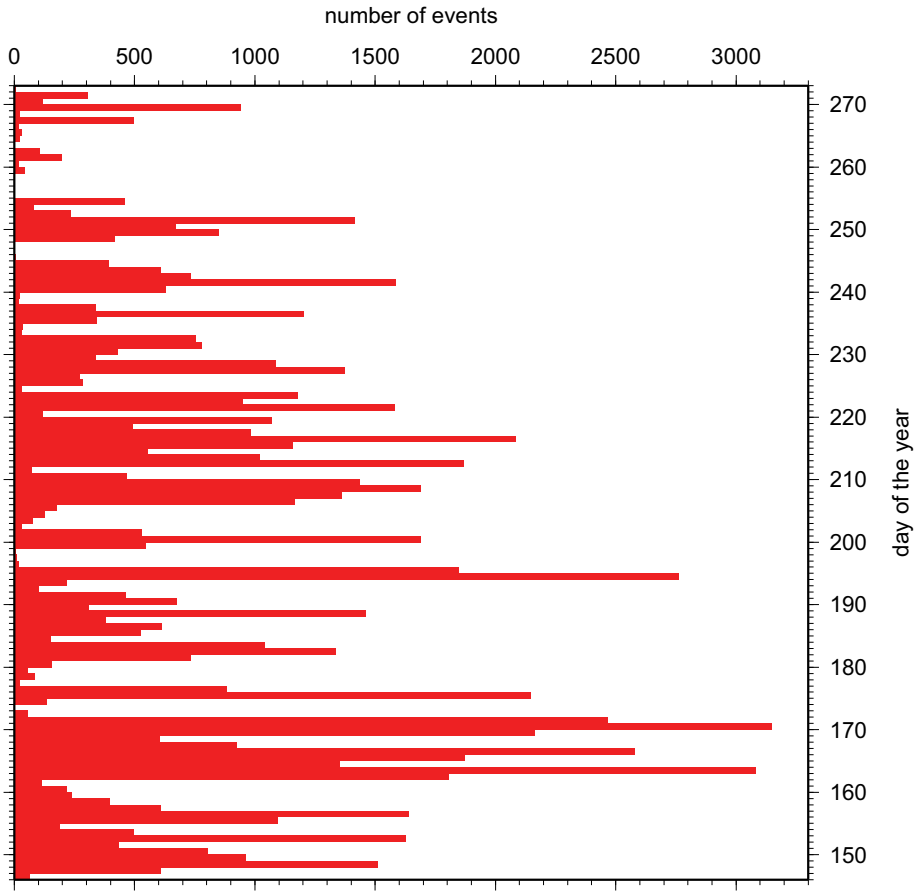

Fig. 6.4.4. Number of northcoast-events per day of the major subgroup (purple dots in 6.4.2).

In Fig. 6.4.5, the absolute occurrence of events per hour and the mean/median of events is plotted against the wind direction. It is slightly evident that there are more events observed when the wind comes from the north. The correlation suggests a dependency of the recorded signals with weather phenomena.

There is a strong connection between the mean amplitude at all stations, measured for ten minutes at the beginning of each hour at the vertical components, and the wind speed of the corresponding hour (Fig. 6.4.5). The mean amplitude is a measure of the noise at the stations. Hence, the noise increases with increasing wind speed and possible occurring events may not be observed, so that the actual temporal distribution is distorted. The number of events decreases with increasing wind speed (Fig. 6.4.5). This way, it is difficult to identify the real

cause of the events at the northern coast because every possible relation is overlaid by the noise level due to wind speed.

It was assumed that the events occur due to waves breaking at the steep coast but measurements of the wave height are of no good quality and information about the wave direction are not available. There is no apparent relationship between the wave heights and the number of events for the major subgroup (purple dots in Fig. 6.4.2) but there can be observed a clear correlation (Fig. 6.4.5) for one of the subgroup with less detected events (orange dots in Fig. 6.4.2). The inter-event times between two successive events of the northern signals do not seem to have a characteristic period that would point towards pounding of the waves against the shore line.

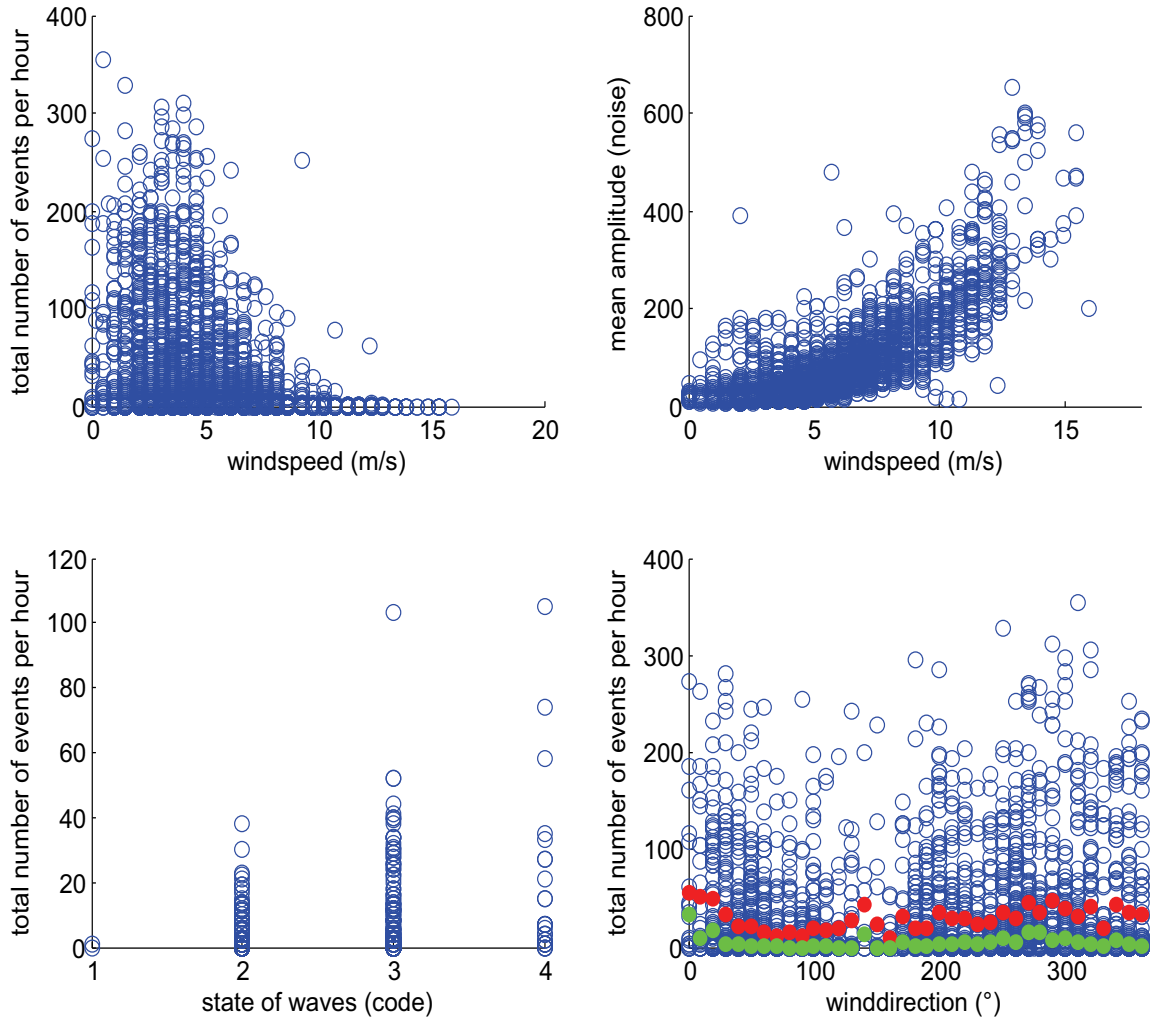

Fig. 6.4.5. Northcoast events. Correlations between: (top left) number of events and wind speed for the largest event group (purple dots in Fig. 6.4.2), (top right) wind speed and noise level at the traces, (bottom left) state of waves and the number of events for the smaller group of events (orange dots in Fig. 6.4.2) and (bottom right) the wind direction and the number of events for the largest event group (purple dots in Fig. 6.4.2). The red and green dots display the mean and median of the number of events, respectively. Code wave heights: 1: 0-0.1 m, 2: 0.1-0.5 m, 3: 0.5-1.25 m, 4: 1.25-2.5 m, 5: 2.5-4 m.

Events inside the network

A second group of events appeared at the beginning of the recording time (see green dots in Fig. 6.4.2). The signals can be located at different positions between the stations of the network often corresponding with the locations of rivers and lakes on the island. They are characterized by strong signal amplitudes at the stations closest to the source origin and no recordings at seismometers at greater distance. In most of the cases just surface waves can be observed, indicating very shallow sources.

It is assumed that this group occurs due to melting snow and the breaking of ice floes on the rivers and lakes of the island. The meteorological station on Bear Island reported a thick snow covering until May 29 and a thin snow covering until June 9. Especially at the beginning of June, several events of this kind were recorded, coinciding with a marked rise in the air temperature. It seems to support the aforementioned assumptions of ice and snow melting effects.

Probable tectonic events

Several small events can be found in the dataset with origin in the southern and southwestern parts and surroundings of the island (see yellow dots in Fig. 6.4.2). They were detected at all seismometers of the network but show significant amplitude variations between the stations. The whole seismograms are five to six seconds long. The source signal duration is about one second and has a dominant frequency for the P-phases of about 5 Hz (Fig. 6.4.6). P-, S- and surface-waves could be observed, arriving with incidence angles of about 50º. The strong surface waves indicate shallow source depths, waveform modelling results suggest source depths of less than 1 km. However, the pronounced SH-wave observations of the events do not agree with hypothetical explosion origins. Besides, we have no knowledge about seismic experiments with explosion sources in this area during the occurrence times of these events. Therefore, we assume that these events could have a tectonic origin.

Three different such signals were used as master events for the waveform correlation code to detect other events of the same type. In total 49 events were discovered, about 20 on the same day. We note that the master events were not detected when using one of the other master events as a template. They therefore do not seem to originate from the same or a very close source location (Gibbons & Ringdal, 2006).

A comparison with geological mapped fault structures is not possible. A geological map for Bear Island exists but no information for the closer surroundings of the island are available. Bear Island is located on the sheared continental margin of the Barents Sea shelf. Rifting and breakup of the former continent began in the Late Cretaceous forming the Norwegian-Greenland Sea (Worsley et al., 2001; Breivik et al., 2003; Worsley, 2006; Faleide et al., 2008). The present day stress field of the island is complicated.

It is possible that there are more recorded tectonic events from different locations but it was not feasible to analyze the whole dataset within this study.

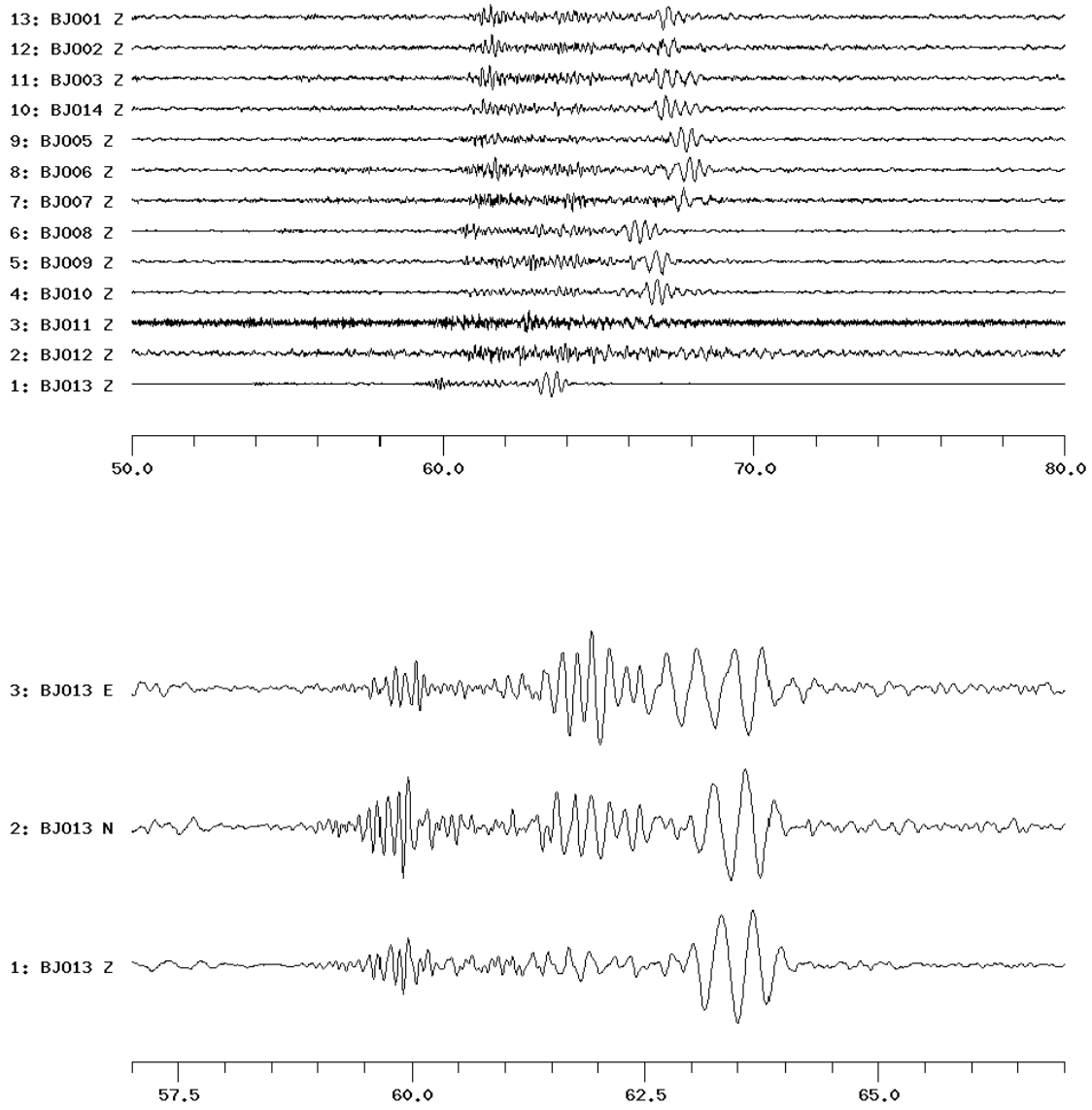

Fig. 6.4.6. Small, most likely tectonic event from August, 4 2008 filtered with a Butterworth band-pass filter from 3-16 Hz. The time axes shows seconds since 11 pm. Top: Vertical components of all stations, absolute amplitudes. Bottom: all three components of station BJO13.

6.4 Conclusions

During the internship, several events could be identified. Weather phenomena, especially the strength of wind, seem to have a great influence on the quality of the recordings in the form of incoherent noise. Other potential noise sources can be found at steep coasts. Although the origin is still in question, such kind of events can disturb the signals of especially smaller tectonic events when occurring in greater numbers. The melting of snow and breaking of ice floes on rivers and lakes acts as a similar noise source in arctic environments.

The presumable tectonic events in the southeast of the array are still under investigation. Signals from events with location estimates will be compared with synthetic seismograms. Depth and kind of source mechanism can be varied until a "best" fitting solution is achieved. A source inversion is planned.

Annabel Händel, University of Potsdam, Germany
Johannes Schweitzer
Frank Krüger, University of Potsdam, Germany

Acknowledgements

The research visit of Annabel Händel at NORSAR was financed by the Transnational Access part of the EC project NERIES (EC Contract Number 026130). The installation and operation of the Bear Island array has been mainly financed by the IPY project "The dynamic continental margin between the Mid-Atlantic-Ridge system (Mohns Ridge, Knipovich Ridge) and the Bear Island region" (Norwegian Research Council Contract Number 176069/S30). The Bear Island array would not have been possible without help and support of our colleagues at the University of Potsdam and at NORSAR during installation and demobilization of the array. The support of the Norwegian Meteorological Institute, Forecasting Division of Northern Norway and the staff of the Meteorological Station on Bear Island is highly acknowledged.

References

Breivik, A.J., Mjelde, R., Grogan, P., Shimamura, H., Murai, Y. & Nishimura, Y. (2003): Crustal structure and transform margin development south of Svalbard based on ocean bottom seismometer data. *Tectonophysics* 369, 37-70.

Czuba, W., Grad, M., Mjelde, R., Guterch, A., Libak, A., Krüger, F., Murai, Y., Schweitzer, J. & the IPY Project Group (2010): Continent-ocean-transition across a rifted shear-margin: off Bear Island, Barents Sea. *Geoph. J. Int.* (revision submitted in June 2010).

Endrun, B., Ohrnberger, M. & Savvaidis, A. (2009): On the repeatability and consistency of three-component ambient vibration array measurements. *Bull. Earthqu. Eng.* **8,** (3), 535-570.

Faleide, J.I., Tsikalas, F., Breivik, A.J., Mjelde, R., Ritzmann, O., Engen, Ø., Wilson, J. & Eldholm, O. (2008): Structure and evolution of the continental margin off Norway and the Barents Sea. *Episodes* **31**, (1), 82-91.

Gibbons, S.J. & Ringdal, F. (2006): The detection of low magnitude seismic events using array-based waveform correlation. *Geophys. J. Int.* **165**, 149-166.

Schweitzer, J. (2001): HYPOSAT – An enhanced routine to locate seismic events. *Pure Appl. Geophys.* **158**, 277-279.

Schweitzer, J. (2002): PD11.1: User Manual for HYPOSAT (including HYPOMOD). In: Bormann, P. (ed.) (2002). *IASPEI New Manual of Seismological Observatory Practice*, GeoForschungsZentrum Potsdam, Vol. 2, 15 pp.

Schweitzer, J. & The IPY Project Consortium Members (2008): The International Polar Year 2007-2008 Project ``The Dynamic Continental Margin Between the Mid-Atlantic-Ridge System (Mohns Ridge, Knipovich Ridge) and the Bear Island Region". *NORSAR Sci. Rep.* **1-2008**, 53-63.

Wathelet, M., Jongmans, D., Ohrnberger, M. & Bonnefoy-Claudet, S. (2008): Array performances for ambient vibrations on a shallow structure and consequences over Vs inversion. *J. Seism.* **12**, (1), 1-19.

Worsley, D., Agdestein, T., Gjelberg, J.G., Kirkemo, K., Mørk, A., Nilsson, I., Olaussen, S., Steel, R.J. & Stemmerik, L. (2001): The geological evolution of Bjørnøya, Arctic Norway: implications for the Barents Shelf. *Norsk Geologisk Tidsskrift* **81**, 195-234.

Worsley, D. (2006): The post-Caledonian geological development of Svalbard and the Barents Sea. *NGF Abstracts and Proceedings* 3, 5-21.